การประดิษฐ์อุปกรณ์ตรวจวัดไอออนโลหะฐานกระดาษที่ตรึงด้วยพอร์ไฟริน

นางสาวจุฑามาศ ปราบพาล

วิทยานิพนธ์นี้เป็นส่วนหนึ่งของการศึกษาตามหลักสูตรปริญญาวิทยาศาสตรมหาบัณฑิต
สาขาวิชาเคมี ภาควิชาเคมี
คณะวิทยาศาสตร์ จุฬาลงกรณ์มหาวิทยาลัย
ปีการศึกษา 2559

FABRICATION OF METAL ION SENSING DEVICES BASED ON PORPHYRIN-IMMOBILIZED PAPERS

Miss Jutamat Prabphal

A Thesis Submitted in Partial Fulfillment of the Requirements
for the Degree of Master of Science Program in Chemistry
Department of Chemistry
Faculty of Science
Chulalongkorn University
Academic Year 2016

Thesis Title	FABRICATION OF METAL ION SENSING DEVICES BASED ON PORPHYRIN-IMMOBILIZED PAPERS
By	Miss Jutamat Prabphal
Field of Study	Chemistry
Thesis Advisor	Assistant Professor Thanit Praneenararat, Ph.D.

Accepted by the Faculty of Science, Chulalongkorn University in Partial Fulfillment of the Requirements for the Master's Degree

.....Dean of the Faculty of Science
(Associate Professor Polkit Sangvanich, Ph.D.)

THESIS COMMITTEE

.....Chairman
(Associate Professor Vudhichai Parasuk, Ph.D.)

.....Thesis Advisor
(Assistant Professor Thanit Praneenararat, Ph.D.)

.....Examiner
(Professor Mongkol Sukwattanasinitt, Ph.D.)

.....External Examiner
(Assistant ProfessorNakorn Niamnont, Ph.D.)

จุฑามาศ ปราบพาล : การประดิษฐ์อุปกรณ์ตรวจวัดไอออนโลหะฐานกระดาษที่ตรึงด้วยพอร์ไฟริน (FABRICATION OF METAL ION SENSING DEVICES BASED ON PORPHYRIN-IMMOBILIZED PAPERS) อ.ที่ปรึกษาวิทยานิพนธ์หลัก: ผศ. ดร.ธนิษฐ์ ปราณีนรารัตน์, 47 หน้า.

ปัญหาการปนเปื้อนของโลหะหนักในแหล่งน้ำเป็นปัญหาที่ส่งผลเสียต่อร่ายกายมนุษย์และสิ่งแวดล้อม เทคนิคที่ใช้ในการตรวจหาโลหะโดยทั่วไปมักมีต้นทุนสูง และต้องการผู้เชี่ยวชาญในการวิเคราะห์ ดังนั้นในปัจจุบันจึงมีการพัฒนาวิธีการตรวจวัดเพื่อทราบชนิดและปริมาณของโลหะที่ถูกลงและใช้งานสะดวกมากขึ้น โดยในงานวิจัยนี้ผู้วิจัยได้ทำการสังเคราะห์และศึกษาความสามารถของการเป็นโพรบในการตรวจวัดไอออนโลหะของอนุพันธ์พอร์ไฟรินที่มีประจุลบ 2 ชนิด ได้แก่ tetrakis(4-sulfonatophenyl)porphyrin (TSPP) และ tetrakis(*N*-methyl-4-pyridyl)porphine tetraiodide (TMPyP) โดยศึกษาการเปลี่ยนแปลงสีและการเรืองแสงของอนุพันธ์พอร์ไฟรินเมื่อมีการจับกับโลหะไอออนชนิดต่างๆ นอกจากนี้ในงานวิจัยนี้ยังได้พัฒนาอุปกรณ์การตรวจวัดโลหะไอออนฐานกระดาษโดยการตรึงด้วยพอร์ไฟริน พบว่า พอร์ไฟรินทั้งสองชนิดสามารถตรวจหา Hg(II) และ Cd(II) ได้จากการเปลี่ยนแปลงสี และตรวจหา Cu(II) ได้จากการดับสัญญาณการเรืองแสงของพอร์ไฟริน อย่างไรก็ตาม เนื่องจาก TSPP มีการเปลี่ยนแปลงสีที่เห็นได้ชัดกว่า ในขณะที่มีวิธีการสังเคราะห์ที่เหมาะสมกับการฝึกปฏิบัติ จึงได้มีการประยุกต์เพื่อฝึกการสังเคราะห์สาร และศึกษาการนำไปใช้งานด้านเคมีวิเคราะห์ของโมเลกุลที่สังเคราะห์ได้ในวิชาเคมีอินทรีย์ปฏิบัติ ในขณะที่ TMPyP ซึ่งมีแรงยึดเหยี่ยวกับผิวกระดาษได้ดีได้ถูกนำไปตรึงบนกระดาษเพื่อประดิษฐ์อุปกรณ์ตรวจวัดปริมาณ Cu(II) และพบว่ามีขีดจำกัดการตรวจวัดเท่ากับ 2.41 ไมโครโมลาร์ และสามารถวิเคราะห์ปริมาณ Cu(II) ในน้ำดื่มตัวอย่างและน้ำประปาโดยมีค่าการได้กลับคืนของปริมาณไอออนทองแดงอยู่ระหว่างร้อยละ 94-100 นอกจากนี้ยังได้ทำการพัฒนาอุปกรณ์ฐานกระดาษเพื่อตรวจวัดปริมาณ Cu(II) โดยอาศัยการวัดระยะทาง (distance-based microfluidic paper devices) ที่สามารถตรวจวัดปริมาณ Cu(II) ในช่วง 13- 57 ไมโครโมลาร์อีกด้วย

ภาควิชา เคมี ลายมือชื่อนิสิต .....

สาขาวิชา เคมี ลายมือชื่อ อ.ที่ปรึกษาหลัก .....

ปีการศึกษา 2559

5771945823 : MAJOR CHEMISTRY

KEYWORDS: PORPHYRINS / PAPER-BASED DEVICES

JUTAMAT PRABPHAL: FABRICATION OF METAL ION SENSING DEVICES BASED ON PORPHYRIN-IMMOBILIZED PAPERS. ADVISOR: ASST. PROF. THANIT PRANEENARARAT, Ph.D., 47 pp.

Contaminations of heavy metals in water sources can pose serious hazards to human health and the environments. Commercially available techniques are usually expensive and require highly skilled operators. Thus, inexpensive and simple sensing devices for monitoring heavy metals have been developed in recent years. In this research, charged porphyrins including tetrakis(4-sulfonatophenyl)porphyrin (TSPP) and tetrakis(*N*-methyl-4-pyridyl)porphine tetraiodide (TMPyP) were synthesized and investigated for their abilities as sensors for metal ions *via* UV-vis absorption and fluorescence modes of detection. Furthermore, these molecules were also deposited on paper support to evaluate their abilities as paper-based sensors. It was found that both porphyrins could detect Hg^{2+} and Cd^{2+} *via* colorimetric changes, while both could sense Cu^{2+} *via* the reduction of fluorescence signals. However, due to the clearer color changes of TSPP and simpler synthetic methods, the molecule was selected as an exemplary module for integration between organic synthesis and real-world analytical applications in practical organic chemistry course. On the other hand, TMPyP, with its stronger interaction with cellulose surface, was fabricated as a more ready-to-use paper-based Cu^{2+} sensing device. This device was found to be able to sense Cu^{2+} with a limit of detection of 2.41 μM, and could be used to analyze Cu^{2+} in commercial drinking waters and tap water with the percent recovery in the range of 94-100%. Moreover, distance-based microfluidic paper devices based on fluorescence quenching were also developed – this could sense Cu^{2+} in the range of 13-57 μM.

Department: Chemistry Student's Signature .....

Field of Study: Chemistry Advisor's Signature .....

Academic Year: 2016

ACKNOWLEDGEMENTS

Firstly, I would like to thank my thesis advisor Assistant Professor Dr. Thanit Praneenararat of the Department of chemistry, Faculty of Science, Chulalongkorn University for his support and motivation. His guidance and his encouragement always make me feel warm since the beginning of my research to present.

My sincere thank also go to my thesis committee: Associate Professor Dr. Vudhichai Parasuk, Professor Dr. Mongkol Sukwattanasinitt and Assistant Professor Dr. Nakorn Niamnont. I am gratefully in indebted to them for their very valuable questions and comments on this thesis.

Finally, I must express my bottomless thanks to my family, my friends and all members in TP labs for providing me with continuous support throughout many years of the study. This accomplishment would not have been possible without them. Thank you.

CONTENTS

Page

Page

LIST OF FIGURES

LIST OF SCHEMES

LIST OF TABLES

LIST OF ABBREVIATIONS

AAS	atomic absorption spectroscopy
calcd	calculated
$CDCl_3$	deuterated chloroform
DMG	dimethylglyoxime
DMSO-d_6	deuterated dimethyl formamide
δ	chemical shift
HEPES	4-(2-hydroxyethyl)-1-piperazineethanesulfonic acid
ICP-AES	inductively-coupled plasma atomic emission spectroscopy
ICP-MS	inductively-coupled plasma mass spectrometry
J	coupling constant
m/z	mass-to-charge ratio
MHz	megahertz
MS	mass spectrometry
NMR	Nuclear Magnetic Resonance spectroscopy
PADs	Paper-based analytical device
ppm	part per million
TMPyP	tetrakis(*N*-methyl-4-pyridinyl)porphine tetraiodide
TPP	5,10,15,20-tetraphenylporphyrin
TPyP	5,10,15,20-tetrakis(4-pyridinyl)porphyrin
TSPP	tetrakis(4-sulfonatophenyl)porphyrin
UV-vis	ultraviolet-visible

λ	wavelength
λ_{ex}	excitation wavelength
λ_{max}	maximum absorption wavelength
µL	microliter(s)

CHAPTER I
INTRODUCTION

1.1 Heavy metals pollutions

Heavy metals were heavily used in various industrial productions such as electronics and plastics although these metals were known to have serious hazards on human's health and the environment. Mercury is well known as a toxic metal that can be accumulated in several organisms in the food chain such as fish, which will finally get into humans. Chronic poisoning of mercury can cause damage to central nervous system and lead to several symptoms such as dysarthria, movement disorder, mental deterioration and Minamata disease.[1] Cadmium is also a seriously toxic and carcinogenic metal that can be found from electroplated steel, plastic pigment and electronic batteries. Cadmium exposure can increase the risk of cardiovascular disease, cancer, and damage to kidneys and skeletons.[2] Copper is an essential nutrient but a high level of copper also is also toxic. High intake of copper is a risk factor for diabetes mellitus, neurodegenerative disease and arteriosclerotic vascular disease.[3] As a first measure, the ability to detect and quantify these metals would be beneficial for the overall management.

1.2 Paper-based heavy metals sensors

Currently, several analytical methods for heavy metal detections that are highly efficient, sensitive and rapid have been developed. The most common methods include atomic absorption spectroscopy (AAS), inductively-coupled plasma atomic emission spectroscopy (ICP-AES), inductively-coupled plasma mass spectrometry (ICP-MS), and potentiometry. [4] However, the majority of these methods requires highly skilled operators, extensive sample preparations and established locations making on-site testing improbable. Thus, simple, inexpensive and field-based sensing devices recognizing heavy metals were developed in recent years. [5-8] Most devices focused on a simple readout such as colorimetric (naked-eye) changes [9-10] and fluorescence from an excitation *via* a commercially available black light. [11] The sensors usually needed organic chromophores that can coordinate to transition metals with concomitant

spectroscopic changes. Moreover, some of recent studies also embedded or immobilized these molecules on solid supports to enhance its versatility and applicability. [12-13]

Paper-based analytical device (PADs) were developed and gained popularity due to several advantages such as light weight, low cost and little consumption of samples.[6] In addition, paper contains hydroxy groups that can be used to react with a variety of organic molecules, thus broadening the scope of immobilization. Generally, colorimetric detection was used for a qualitive analysis that can identify the presence of analyte in the sample. On the other hand, quantitative analysis can be done with additional signal readout such as the measurement of the color intensity and conversion to numerical data with imaging software.[9] Moreover, hydrophobic barrier such as waxes and marker inks were used to create patterns on paper devices for controlled testing area and increased analytical reproducibility. [14-15]

For example, quantitative colorimetric paper-based analytical device was prepared by printing waxes to create text-reporting patterns for heavy metals (**Figure 1.1A**). In this study, chromophores that are able to give specific color changes for each metal were immobilized onto patterned paper by physical adsorption.[9] To evaluate the concentrations of metals, photo scanner was used to collect images. Computer software was used to convert the color intensity to numerical data for establishing calibration curves for quantification. The application of text-reporting paper device was performed by simply dipping into water samples and the color change of corresponding metals were shown instantaneously (**Figure 1.1B**). The detection limits of Cr(VI), Ni(II) and Cu(II) were determined to be 9.6×10^{-6} M, 8.5×10^{-6} M and 1.3×10^{-6} M respectively.

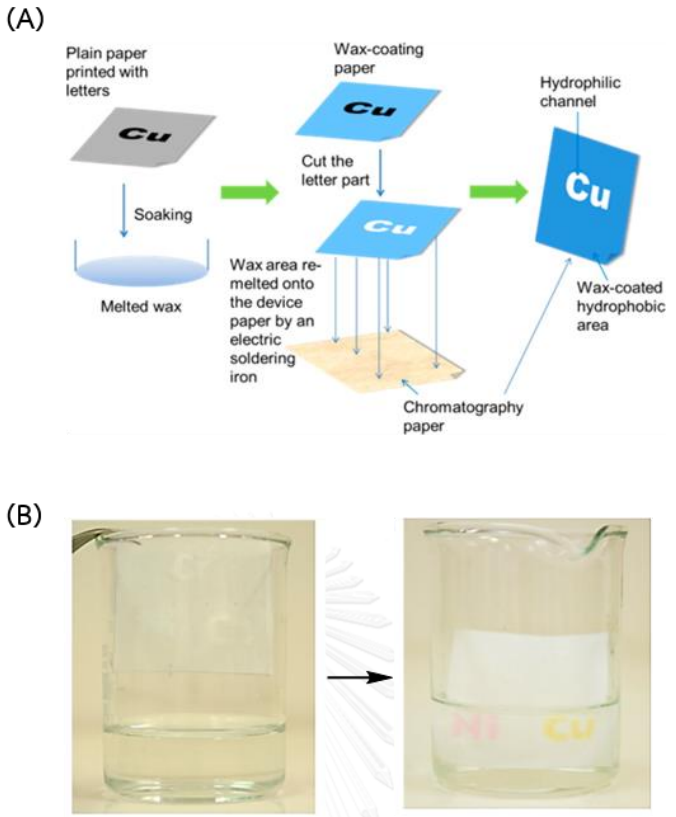

Figure 1.1 (A) Schematic of the fabrication of text-reporting patterned paper device. (B) Application of the paper device in a simulated waste water.[9]

Another example is the development of a colorimetric paper-based device to measure metal-containing aerosols.[6] The device pattern consisted of a sample reservoir, a pre-treatment zone and a detection zone containing reagent for the determination of the amounts of Fe, Cu and Ni (**Figure 1.2A**). Reagents in the pretreatment zone was used to adjust conditions that are suitable for target metal binding with reagents in the detection zone. To determine the amount of metals, the converted grey intensity of colors in the detection zone was measured by imaging software and used to generate calibration curves. The application of this device was performed by placing the digested sample punch on the sample reservoir. This followed by an addition of water, resulting in the metal ions being transported to the detection reservoir (**Figure 1.2B**). The detection limits of Fe, Cu and Ni were determined to be 1.5 μg, 1 μg, and 1 μg respectively.

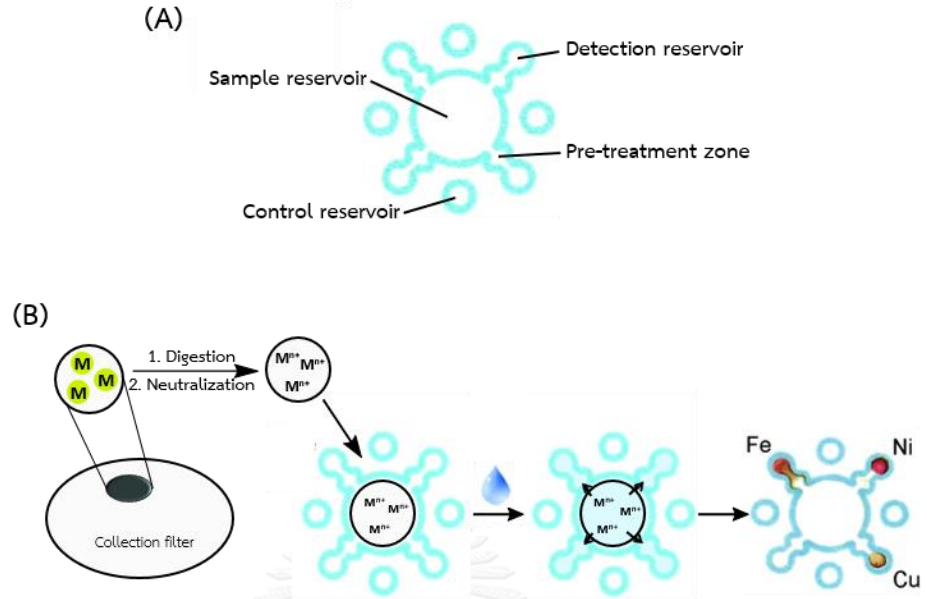

Figure 1.2 (A) The pattern of a microfluidic paper-based device by Mentele *et al*. (B) Application procedure of the paper-based device.[6]

1.3 Distance-based microfluidic device

The use of a photo scanner and imaging software can improve the accuracy and the sensitivity of quantitative analysis, but this also increases the analysis cost and could limit the amenability for on-site testing. Therefore, simpler methods for quantitative analysis without using other devices are needed. Distance-based microfluidic device was developed to collect quantitative data without the need to digitize data.[16-18] For instance, the measurement of the distance having color change could be achieved by depositing sensoring molecules along a narrow channel. Thereafter, an analyte was allowed to flow in this channel to cause color changes. Quantification was achieved by measuring the length of new color. The amount of analyte was determined by measuring the length of color without using computer analysis.[19]

Cate and co-workers developed a distance-based microfluidic device to quantify the nickel level in incineration ash sample using complexation between Ni^{2+}

and dimethylglyoxime.[16] The hydrophobic microchannel was designed using graphic software and printed onto cellulosic filter paper using wax ink (**Figure 1.3A**). Dimethylglyoxime (DMG) reagent was deposited along the channel by nebulizer then a masking tape was applied to the back side to prevent sample leaking. Red color was generated from Ni^{2+}-DMG complex and the distance of the color depended on the amount of Ni^{2+} in sample (**Figure 1.3B**).

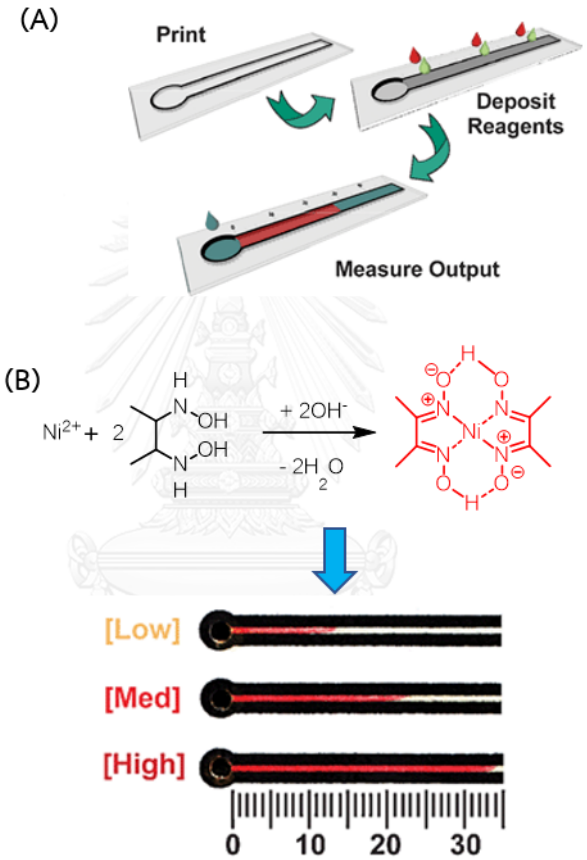

Figure 1.3 (A) Schematic of distance-based detection. (B) Formation of Ni^{2+}-DMG complex to create red color along detection channel.[16]

An example is about the development of a distance-based paper device for quantification three metals. In this research, paper device was fabricated using wax printing to create hydrophobic patterns (**Figure 1.4A**).[18] The colorimetric reagent, a buffer, and masking agents were deposited by inkjet printer to the desired areas.

Moreover, a colorimetric indicator was used to estimate timing of reaction process (**Figure 1.4B**). The results showed the detection limit of Ni(II), Fe(II), and Cu(II) of 5 ppm, 1 ppm and 5 ppm respectively.

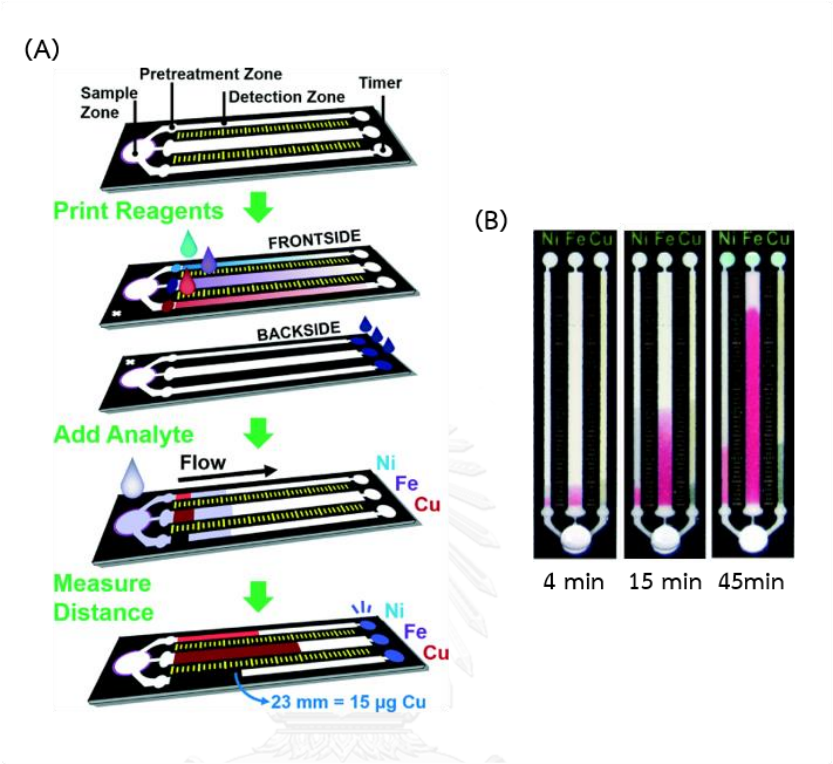

Figure 1.4 (A) Schematic of the fabrication of multiplex paper device.

(B) Application of paper device with timing indicator.[18]

1.4 Porphyrins

Among the diverse class of organic chromophores, porphyrins are an interesting class of chromophores that can give spectroscopic changes depending on the central metal. Porphyrins are macrocyclic aromatic compounds that can be found in many important biological systems such as chlorophyll, cytochrome C and heme B (**Figure 1.5**).[20] Porphyrin is a promising signaling unit due to its photophysical characteristics such as high extinction coefficient and tunable fluorescence emission. The central tetrapyrrole of porphyrins is able to form complexes with a variety of metal ions. Recent works showed that some charged porphyrins exhibited colorimetric changes that could be detected by naked eyes.[10, 21]

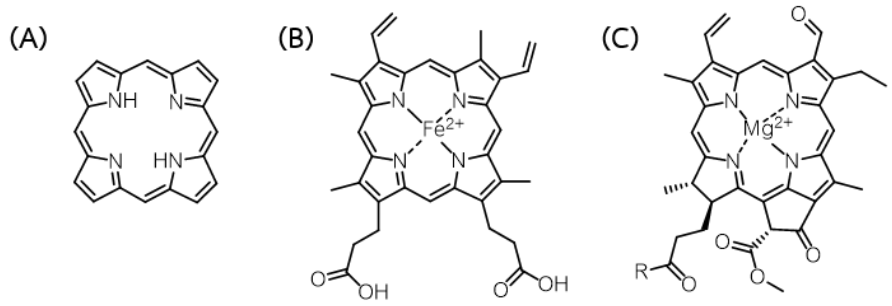

Figure 1.5 Structure of (A) Porphine, (B) Heme, (C) Chlorophyll

Due to the aforementioned advantages, charged porphyrins have been utilized in metals sensing applications. For example, positively charged porphyrins (**TMPyP**) were immobilized on to modified surface silica monolith by electrostatic force (**Figure 1.5B**).[21] The color of the sensor was changed due to the binding of **TMPyP** with cadmium (II) ion with the response time of 5 minutes (**Figure 1.4B**). The porphyrin grafted silica sensor showed good sensitivity to cadmium (II) ion, with the detection limit of 7.0×10^{-9} M.

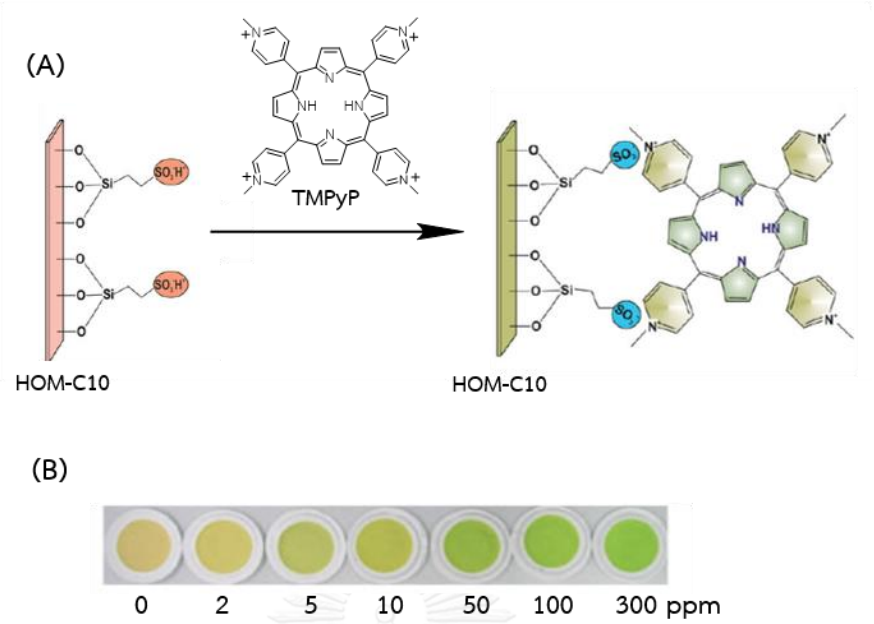

Figure 1.6 (A) Schematic of **TMPyP** immobilized on the surface of modified silica monolith; (B) The colorimetric responses of **TMPyP** to various concentrations of cadmium (II) ions.[21]

1.5 Objective of work

The aim was to synthesize and immobilize charged porphyrins through a physical adsorption on paper. Thereafter, paper-based analytical devices were developed to sense metal ions *via* both colorimetric and fluorescence detection methods, with an aim of obtaining inexpensive, portable and sufficiently sensitive sensors.

CHAPTER II

EXPERIMENT

2.1 Materials and Chemicals

All chemicals and reagents were purchased from Acros organic, Fluka, Merck, UNILAB and Sigma-Aldrich Co., Ltd. All solvents were purchased from RCI Labscan (Thailand) and used without further purification. Milli-Q water was obtained from ultrapure water system with millipak® 40 filter unit 0.22 µm, Millipore (USA). Whatman No. 1 Chromatography paper was purchased from GE Healthcare UK Ltd. ColorQube 8580 Solid ink color printer was purchased from Xerox®.

2.2 Syntheses of porphyrin derivatives as metal ion sensors

2.2.1 Synthesis of 5,10,15,20-tetraphenylporphyrin (TPP)

Freshly distilled pyrrole (1.11 mL, 16 mmol) and benzaldehyde (1.63 mL, 16 mmol) were refluxed in 40-mL propionic acid for 30 min (**Scheme 2.1**).[22] The reaction was cooled down to room temperature. The mixture was filtered off and washed several times with methanol to give 5,10,15,20-tetraphenylporphyrin (**TPP**) as a purple solid in 644 mg (26 %yield). ^{1}H NMR (400 MHz, $CDCl_3$) **δ** 8.87 (s, 8H), 8.25 (d, ***J*** =7.2 Hz, 8H), 7.78 (m, 12H), -2.74 (s, 2H). ^{13}C NMR (100 MHz, $CDCl_3$) **δ** 142.06, 134.41, 130.98, 127.55, 126.52, 120.00.

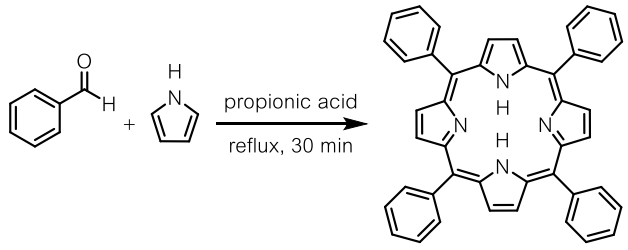

TPP

Scheme 2.1 Synthesis of 5,10,15,20-tetraphenylporphyrin (TPP)

2.2.2 Synthesis of tetrakis(4-sulfonatophenyl)porphyrin (TSPP)

Synthesis of **TSPP** was carried out *via* sulfonation reaction of **TPP**. **TPP** (100 mg, 0.16 mmol) and 5-mL concentrated sulfuric acid were ground by a glass rod to

become homogeneous paste, which was then heated at 140 °C for 4 hours (**Scheme 2.2**).[23] The solution was cooled down to room temperature and added with 25-mL deionized water. The mixture was filtered off and washed with water several times. The filtrate was diluted with deionized water approximately 100 mL and adjusted to pH 8 by 10 M NaOH. After the removal of the solvent, the crude product was re-dissolved by methanol and filtered to remove inorganic salts. The filtrate was dried to give tetrakis(4-sulfonatophenyl)porphyrin (**TSPP**) as a purple solid in 142 mg (85 %yield). ^{1}H NMR (400 MHz, DMSO-d_6) **δ** 8.87 (s, 8H), 8.22 (d, ***J*** = 7.9 Hz, 8H), 8.09 (d, ***J*** = 7.8 Hz, 8H), -2.91 (s, 2H). ^{13}C NMR (100 MHz, DMSO-d_6) **δ** 147.31, 140.94, 133.28, 131.04, 123.81, 119.29. ESI-MS: m/z calcd for $C_{44}H_{26}N_4O_{12}S_4^{4-}$ [M^{4-}] 232.511, found 232.878.

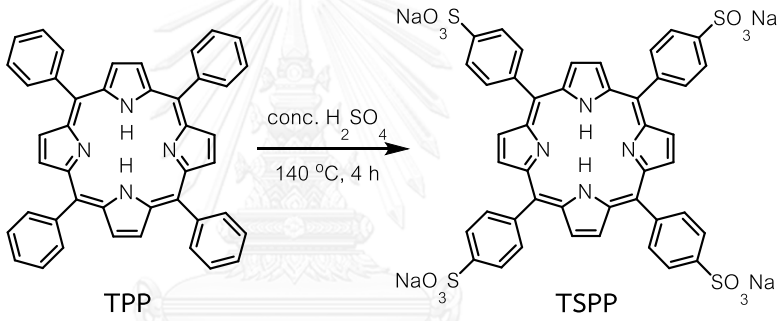

Scheme 2.2 Synthesis of tetrakis(4-sulfonatophenyl)porphyrin (**TSPP**)

2.2.3 Synthesis of 5,10,15,20-tetrakis(4-pyridinyl)porphyrin (TPyP)

Freshly distilled pyrrole (1.11 mL, 16 mmol) and 4-pyridinecarboxaldehyde (1.50 mL, 16 mmol) were refluxed for 1 hour in 40-mL propionic acid. After the reaction was cooled and diluted with deionized water (1:1), the mixture was left in a refrigerator for 10 hours. Finally, the mixture was filtered off and washed with deionized water until the filtrate became colorless and odorless. The product was dried to give a dark purple solid (416 mg, 17%). ^{1}H NMR (400 MHz, $CDCl_3$) **δ** 9.07 (d, ***J*** = 4.6 Hz, 8H), 8.87, (s, 8H) 8.17(d, ***J*** = 4.5 Hz, 8H), -2.93 (s, 2H). ^{13}C NMR (100 MHz, $CDCl_3$) **δ** 150.02, 148.52, 129.89, 129.49.

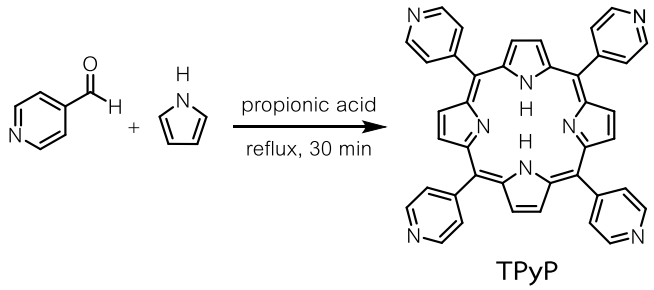

Scheme 2.3 Synthesis of 5,10,15,20-tetrakis(4-pyridinyl)porphyrin (**TPyP**)

2.2.4 Synthesis of tetrakis(*N*-methyl-4-pyridinyl)porphine tetraiodide (TMPyP)

Methylation of tetrakis(4-pyridinyl)porphyrin was achieved as following**. TPyP** (100 g, 0.16 mmol) and methyl iodide (0.6 mL, 9.6 mmol) were dissolved in 8-mL DMF, and the mixture was refluxed for 1 hour.[24] After the mixture was cooled, 10-mL acetone was added to cause precipitation of the product. The precipitate was filtered off and washed with acetone until the washing solution became colorless. **TMPyP** was obtained as dark brown solid in 178 mg (93 %yield). ^{1}H NMR (400 MHz, DMSO-d_6) **δ** 9.50 (d, ***J*** =5.8 Hz, 8H), 9.21 (s, 8H), 9.01 (d, ***J*** =5.5 Hz, 8H), 4.73 (s, 12H), -3.10 (s, 2H). ^{13}C NMR (100 MHz, DMSO-d_6) **δ** 156.27, 144.24, 132.07, 115.81, 47.94. ESI-MS: m/z calcd for $C_{43}H_{35}N_8^{3+}$ [(M-CH_3)$^{3+}$] 221.099, found 221.3312.

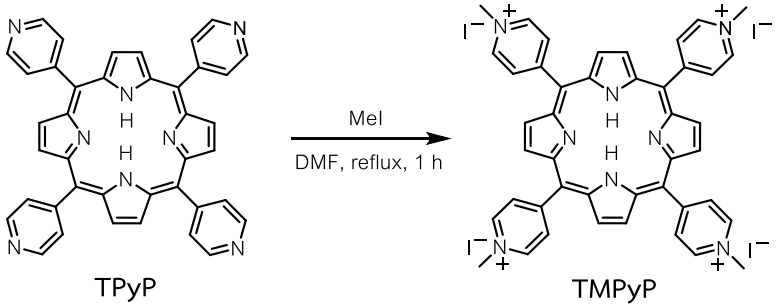

Scheme 2.4 Synthesis of tetrakis(*N*-methyl-4-pyridyl)porphine tetraiodide (**TMPyP**)

2.3 Metal screening tests

Hydrophobic circles were made by using a black permanent maker drawn directly on laboratory filter papers with 5-mm diameter (**Figure 2.1**). **TSPP** or **TMPyP** solution (10 µL of 0.1 mM in 2 mM HEPES buffer, pH 7.5) was separately spotted onto the previously created hydrophobic wells. After the drops were dried, 10 µL of 0.1 mM metal ion solutions (K^+, Na^+, Ca^{2+}, Mg^{2+}, Cr^{3+}, Fe^{2+}, Ni^{2+}, Cu^{2+}, Zn^{2+}, Ag^+, Cd^{2+}, Pb^{2+}, and Hg^{2+}) in 2-mM HEPES buffer were separately dropped onto the previously added **TSPP** or **TMPyP** wells. The results of colorimetric changes were observed instantaneously and the results of fluorescence quenching of were observed under black light (365 nm) after the solutions were dried.

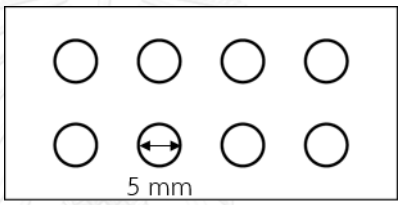

Figure 2.1 Circle patterns for metal screening tests.

2.4 Unknown tests for practical organic chemistry course

Unknown metal samples were prepared to demonstrate the ability of identifying metal ions. Metal ions in each sample are shown in **Table 2.1**, which were prepared in 2 mM HEPES buffer.

Table 2.1 Preparation of unknown metal tests

Sample ID	**Metal ion** (final concentration of each ion = 0.1 mM)
1	Hg^{2+} + Ca^{2+}+ Pb^{2+}
2	Hg^{2+}+ Cu^{2+}
3	Cu^{2+}+ Zn^{2+}
4	Pb^{2+}+ Ca^{2+} +Zn^{2+}

2.5 Sensitivity TMPyP for Cu^{2+} sensor

Hydrophobic patterns with 5-mm diameter were printed on chromatography paper (1Chr) by a Xerox ColorQube 8580 wax printer, and the paper was heated for 30 seconds in an oven at 195 °C to create hydrophobic barriers. Thereafter, the transparent masking tape was applied on the backside of the paper to prevent sample leakage during use. 5 µL of **TMPyP** solution (20 µM in 0.2 M acetate buffer pH 5) was spotted on the created wells. Various concentrations (100 - 1 µM) of Cu^{2+} solution in ultrapure water were dropped onto previously added **TMPyP** wells. After the solution was dried, fluorescence images were taken under the black light (365 nm) by a digital camera (SONY α6000, camera setting: ISO-1250, f/6.3 and 0.6-s exposure time).

2.6 Fabrication of distance-based paper device

The fabrication of distance-based paper device consisted of three steps. First, the thermometer-like pattern was designed with Adobe Illustrator (**Figure 2.2A**) and printed on chromatography paper (1Chr) by a Xerox ColorQube 8580 wax printer. The patterned paper was heated for 30 seconds in an oven at 195 °C, resulting in the wax being melted and penetrated into both sides of the paper. Second, Canon iP2770 inkjet printer was used to print **TMPyP** solution (0.50 mM in 0.2 M acetate buffer pH 5, or in other buffers) on the detection channel (**Figure 2.2B**). lastly, the clear masking tape was applied on the backside of the paper to prevent sample leakage during use.

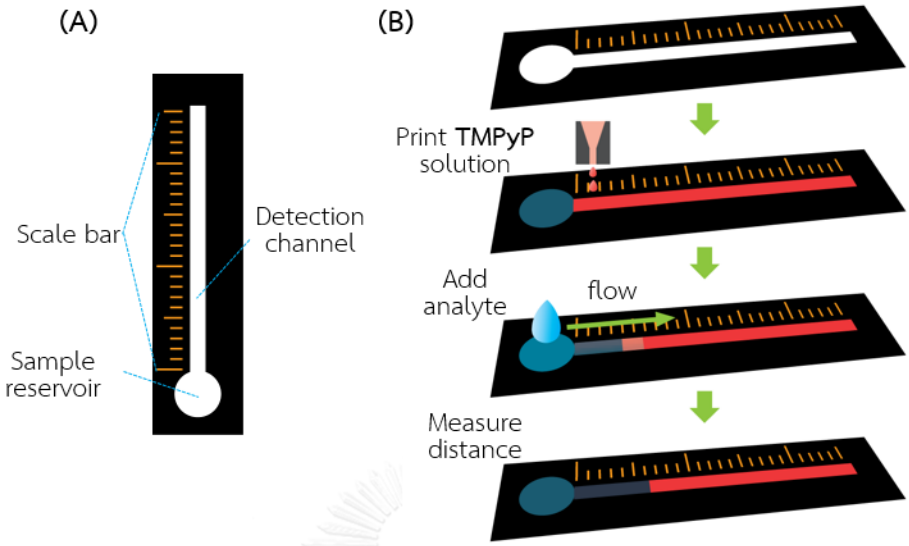

Figure 2.2 (A) Distance-based pattern (B) The layout of sensor fabricated in this study.

CHAPTER III
RESULTS AND DISCUSSION

3.1 Synthesis of heavy metals sensing molecules

Porphyrins is a class of organic compounds that exhibits interesting photophysical properties. Most porphyrins are able to coordinate with metal ions at the center of the porphyrin core. Previous studies showed that charged porphyrins could give discernible spectroscopic changes, which is not always the case for all other porphyrins.[10, 21] In this work, tetrakis(4-sulfonyl)porphyrin (**TSPP**) and tetrakis(*N*-methyl-4-pyridyl)porphyrin (**TMPyP**) were developed for metal ion sensing. The two porphyrins represent different types of charges: **TSPP** contains negative charges, while **TMPyP** contains positive charges. First, **TSPP** was used in simple testing on circle-patterned paper sensor for studies of the colorimetric and fluorometric changes upon contact with various metal ions. Lastly, **TMPyP** was studied for its performance in quantitative analysis and used for fabrication of a microfluidic distance-based paper device in a fluorescence detection mode.

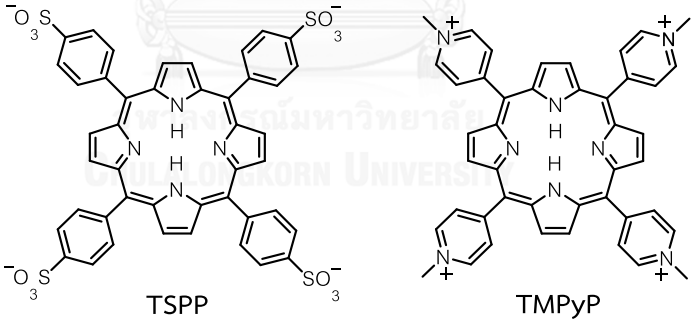

Figure 3.1 The structures of porphyrins used in this study.

3.1.1 Synthesis and Characterizations of 5,10,15,20-tetraphenylporphyrin (TPP)

The synthetic methods of porphyrins have been developed by several research group. The first synthetic method was reported by Rothemund and coworker using the condensation between pyrrole and an aldehyde in methanol.[25] However, the drawback of this method was long reaction time and low yield. Thereafter, Adler and

Longo developed a more efficiency method by refluxing a mixture of pyrrole and an aldehyde in propionic acid under air to obtain **TPP**.[22] Nowadays, the most efficient method was generally accepted to be those reported by Lindsey and coworkers.[26] The porphyrin was formed in two steps. First, the condensation of pyrrole and an appropriate aldehyde in the presence of a Lewis acid under argon gave porphyrinogen. Second, an oxidation with quinone derivatives at room temperature provided the porphyrins. (**Scheme 3.1**)

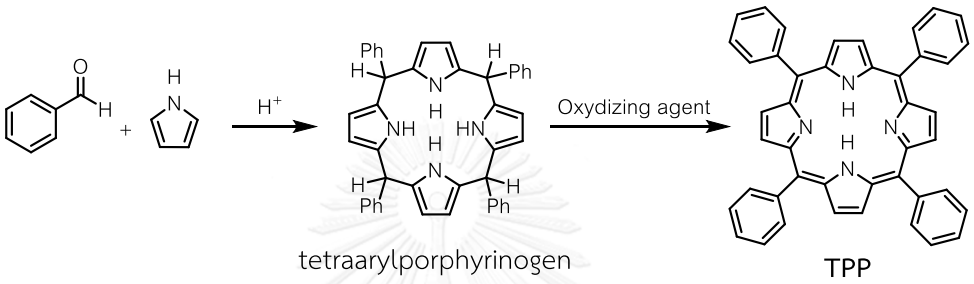

Scheme 3.1 Synthesis of 5,10,15,20-tetraphenylporphyrin (**TPP**) under Linsey's condition.[26]

In this work, the Alder-Longo method was chosen due to simpler reaction and purification requirements for symmetrical porphyrins such as **TPP** and **TPyP** (**Scheme 3.2**)

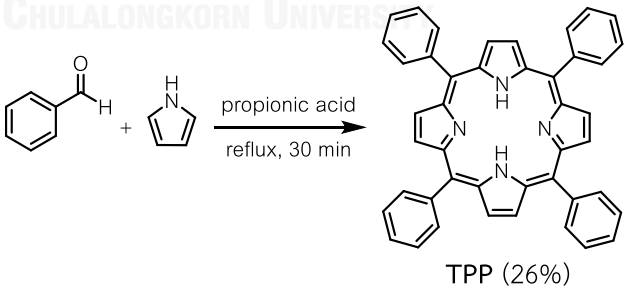

Scheme 3.2 Synthesis of 5,10,15,20-tetraphenylporphyrin (**TPP**)

The cycle of condensation and re-aromatization reaction was repeated with the pyrrole attacking benzaldehyde under an acidic condition (**Scheme 3.3**). Propionic acid was used to increase electrophilicity of benzaldehyde to promote the attack of pyrrole. Re-aromatization occurs easily under this acidic condition to complete each

cycle of the benzaldehyde addition. Thereafter, the tetraarrylporphyrinogen was oxidized by oxygen in air to give **TPP** as a purple solid product in 26 %yield.

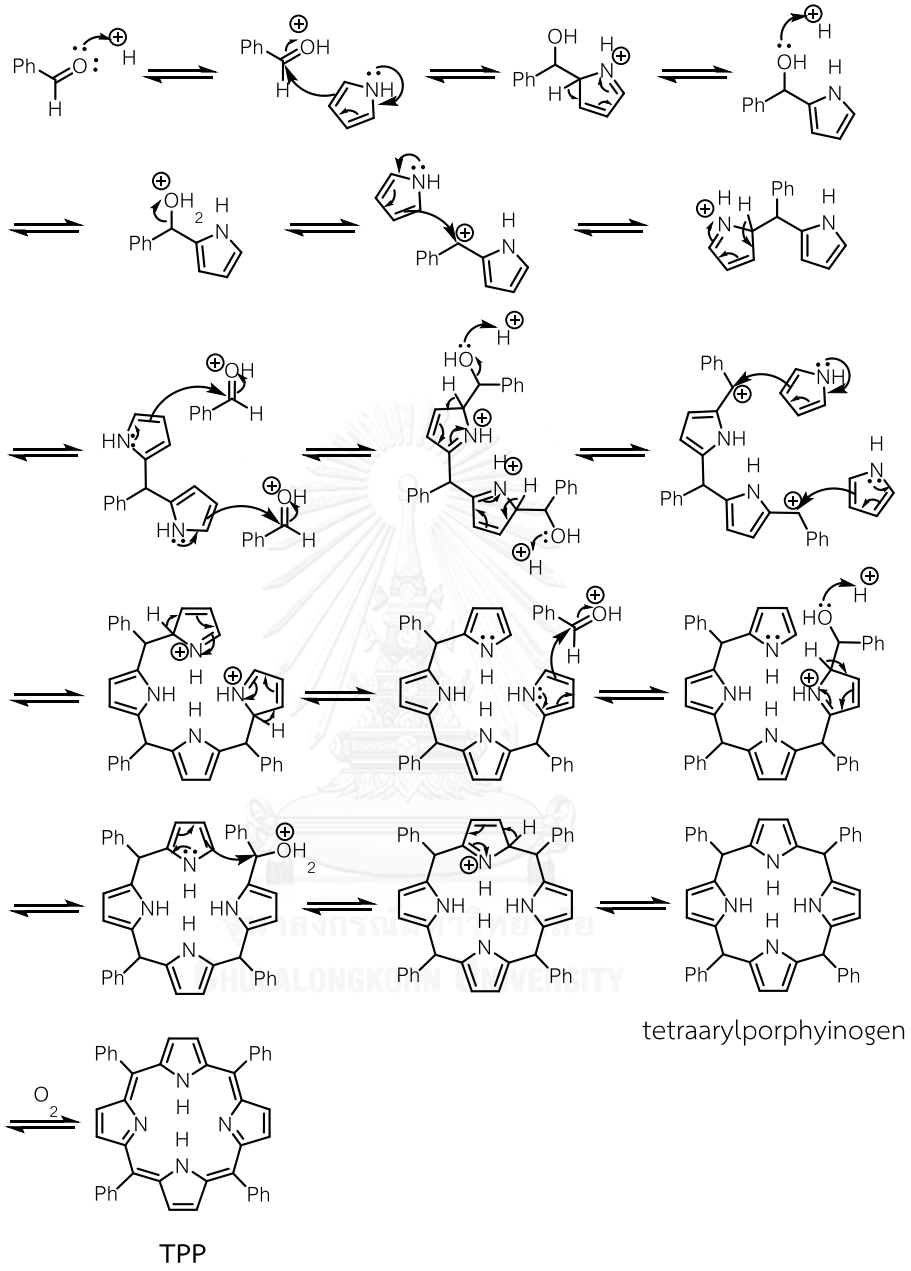

Scheme 3.3 The proposed mechanism of the synthesis of 5,10,15,20-tetraphenylporphyrin (**TPP**)

Base on ^{1}H nuclear magnetic resonance (NMR) spectrum, the characteristic signal of inner protons in the porphyrins ring was observed as a singlet peak at -2.76

ppm (**Figure 3.2**). The protons are highly shielded due to the anisotropic phenomenon. The pyrrolic protons exhibited a sharp singlet signal at 8.87 ppm. Moreover, ^{1}H NMR spectrum showed the ortho protons at 8.25 ppm, and other protons at 7.78 ppm. The ^{13}C NMR did not give much information but could only confirm that there were only aromatic-type carbons in this molecule (**Figure 3.3**).

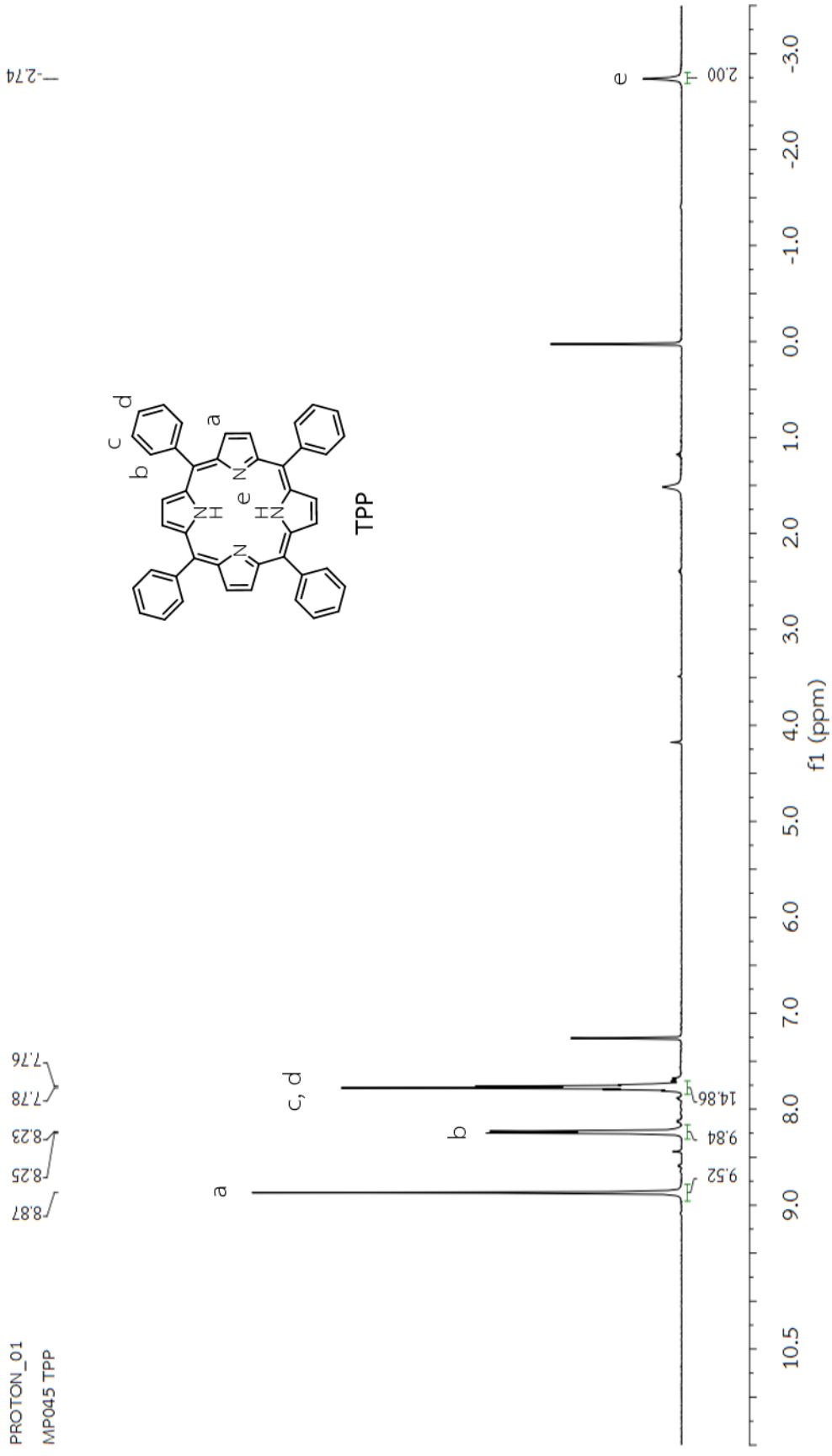

Figure 3.2 ^{1}H NMR of 5,10,15,20-tetraphenylporphyrin (**TPP**) (400 MHz, $CDCl_3$)

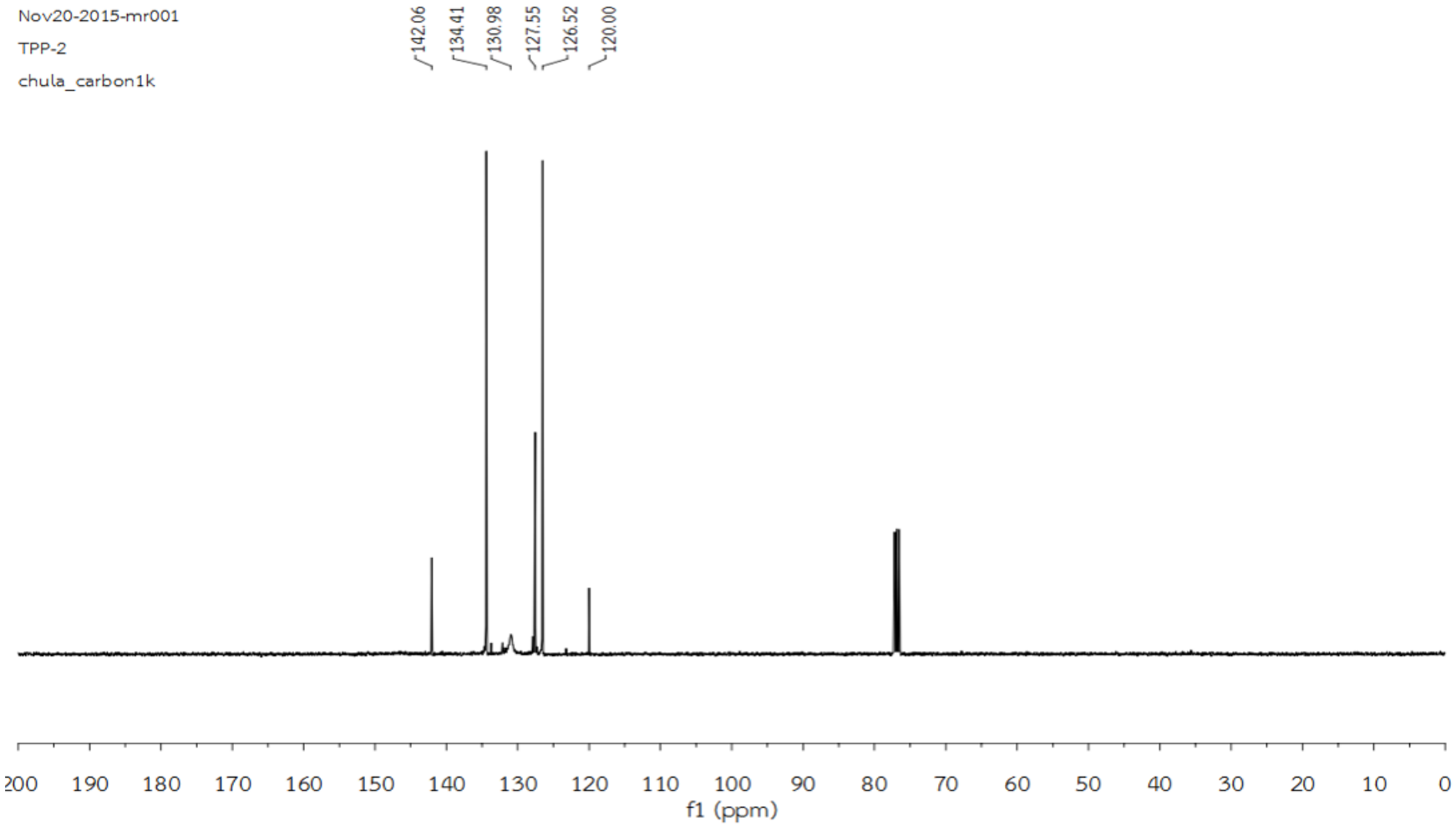

Figure 3.3 ^{13}C NMR of 5,10,15,20-tetraphenylporphyrin (**TPP**) (400 MHz, $CDCl_3$)

3.1.2 Synthesis and Characterizations of tetrakis(4-sulfonatophenyl)porphyrin (TSPP)

TSPP was synthesized *via* sulfonation reaction of **TPP** by using concentrated sulfuric acid as both a reagent and a solvent (**Scheme 3.4**).[23] After neutralization steps, the product was obtained as a sodium salt of **TSPP** in 85 %yield. The ^{1}H NMR spectrum showed relatively similar signal of **TPP** with slightly shifted peak. However, clear doublet signals of meta protons at 8.09 ppm, which demonstrated the success in substitution at para positons (**Figure 3.4**) could be seen. The molecular weight of **TSPP** was confirmed by ESI-MS: [M^{4-}] m/z = 232.878, calcd 232.511 ([M^{4-}] = $C_{44}H_{26}N_4O_{12}S_4^{4-}$) (**Figure 3.6**).

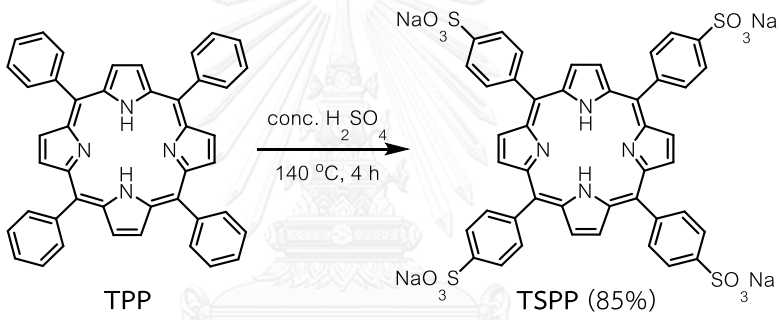

Scheme 3.4 Synthesis of tetrakis(4-sulfonatophenyl)porphyrin (**TSPP**)

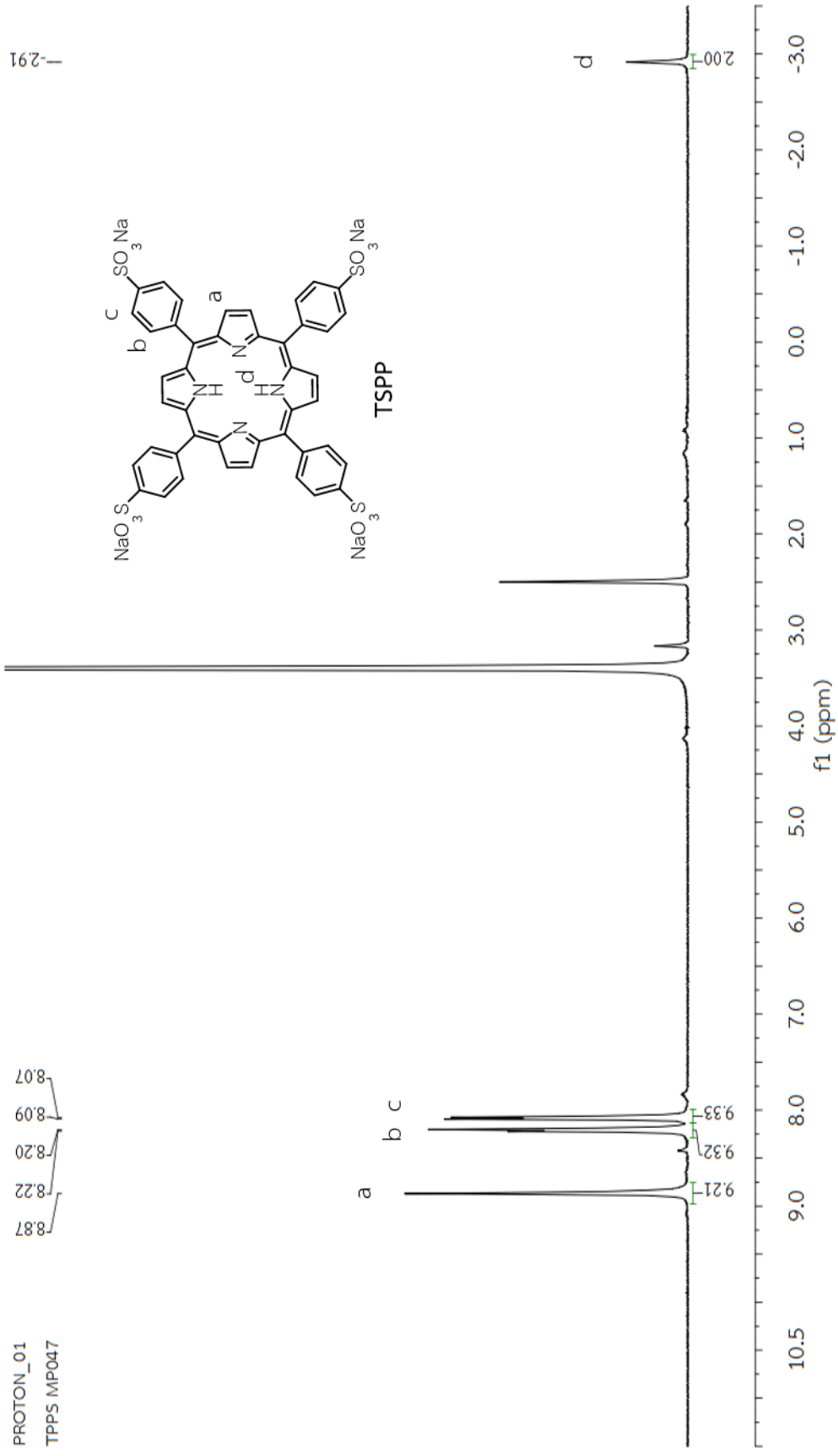

Figure 3.4 ^{1}H MNR of tetrakis(4-sulfonatophenyl)porphyrin (**TSPP**) (400 MHz, DMSO-d_6)

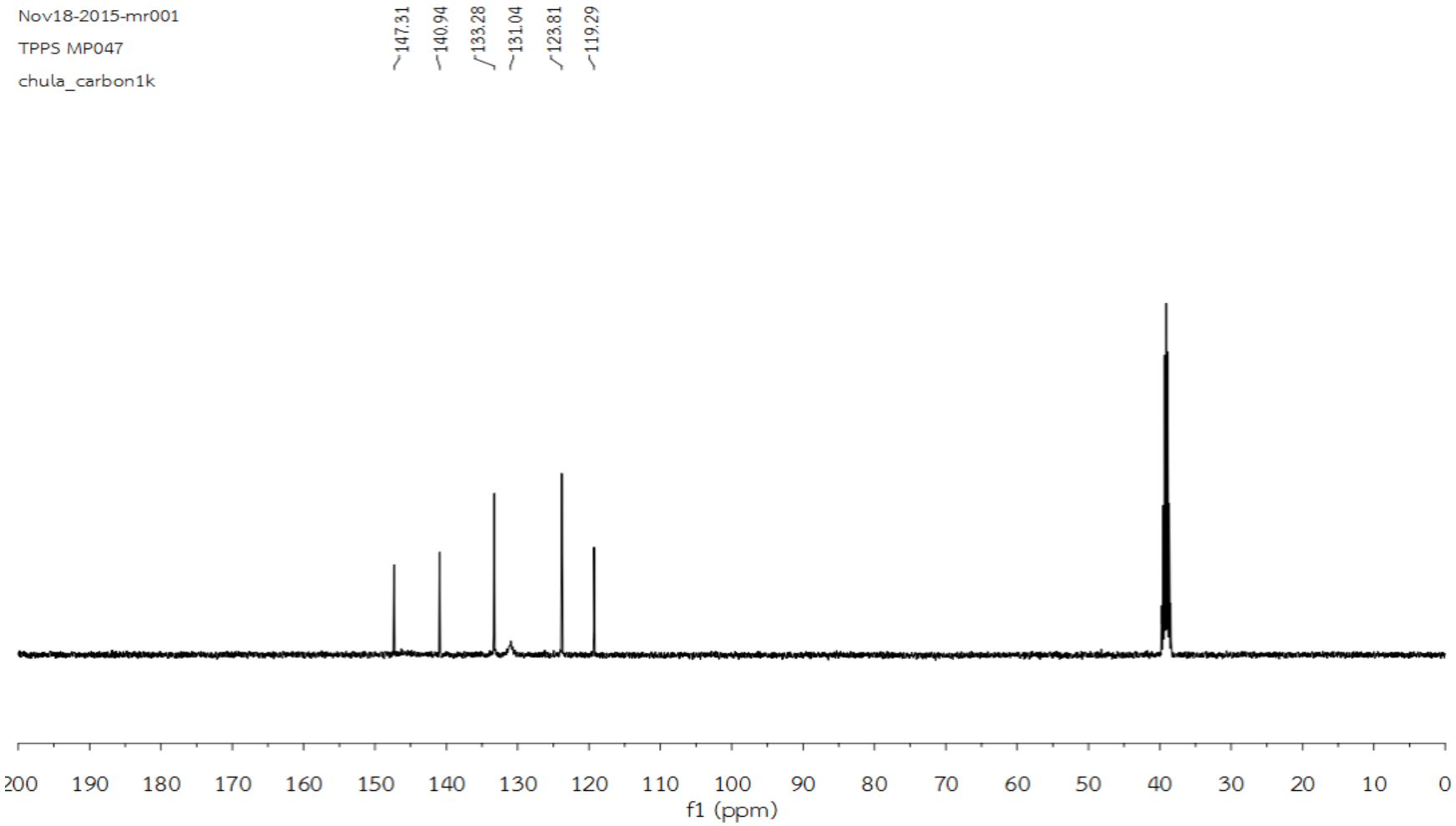

Figure 3.5 ^{13}C MNR of tetrakis(4-sulfonatophenyl)porphyrin (**TSPP**) (400 MHz, DMSO-d_6)

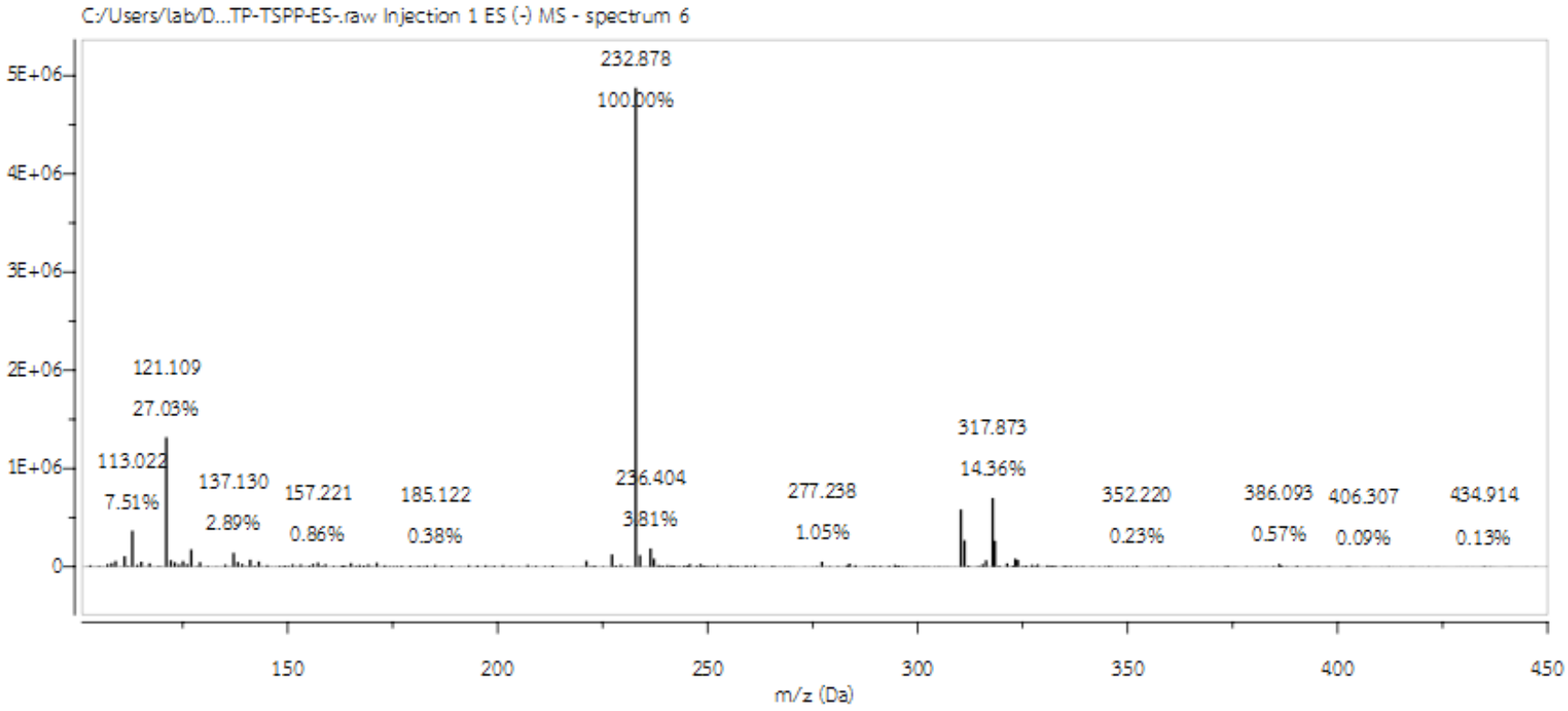

Figure 3.6 Mass spectrum of tetrakis(4-sulfonatophenyl)porphyrin (**TSPP**)

3.1.4 Synthesis and Characterizations of 5,10,15,20-tetrakis(4-pyridinyl)porphyrin (TPyP)

TPyP was obtained from same procedure of **TPP** synthesis (**Scheme 3.5**). After purification process, the product was obtained as a purple solid in 17 %yield. ^{1}H NMR showed a singlet signal of two inner protons at -2.92 ppm and the pyrrolic protons at 8.87 ppm (**Figure 3.7**). Also, the ortho and meta protons of pyridine showed doublet signals at 9.07 and 8.17 ppm respectively.

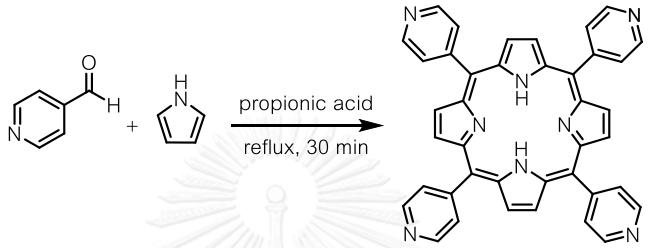

TPyP (17%)

Scheme 3.5 Synthesis of 5,10,15,20-tetrakis(4-pyridinyl)porphyrin (**TPyP**)

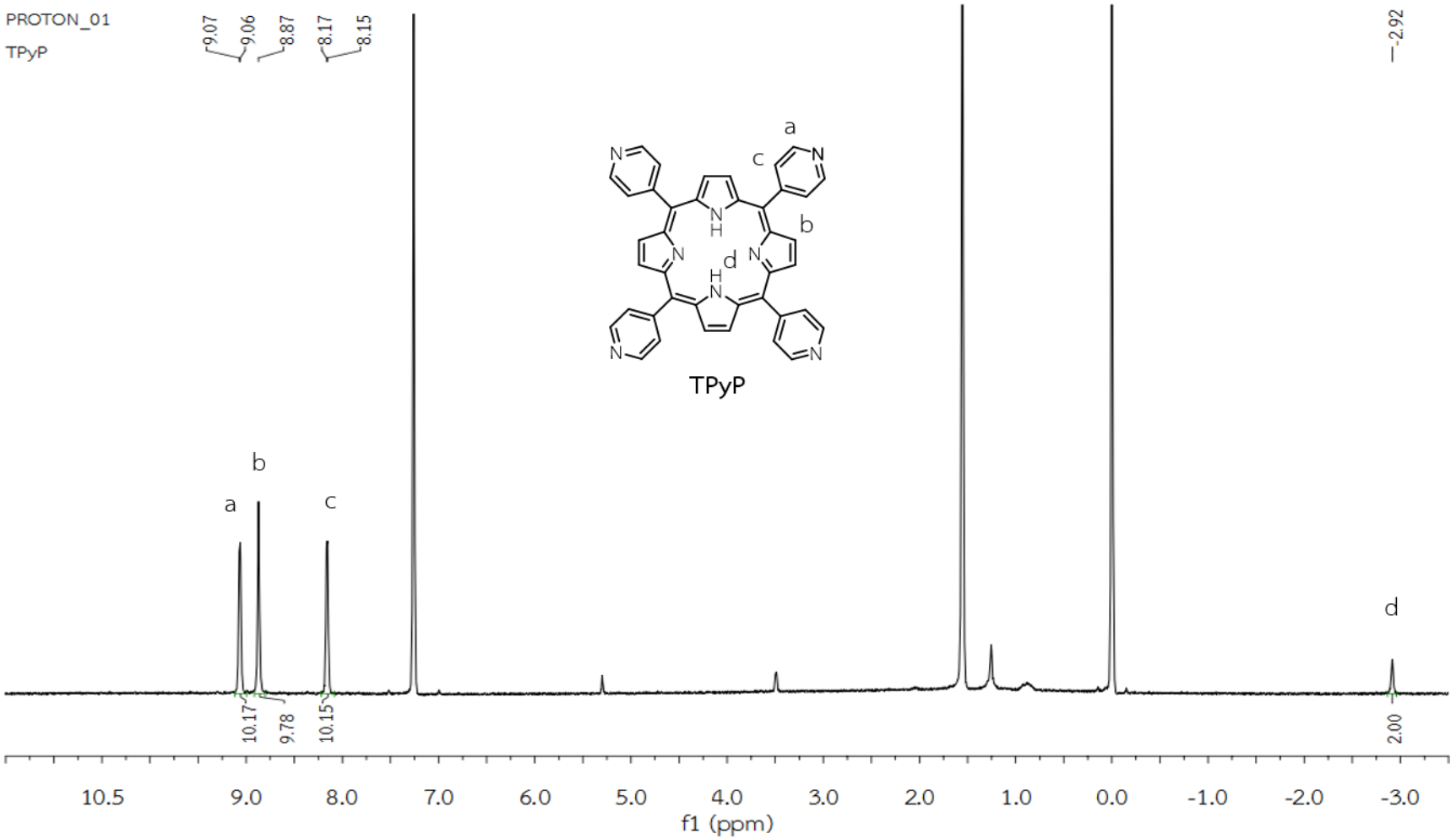

Figure 3.7 ^{1}H MNR of 5,10,15,20-tetrakis(4-pyridinyl)porphyrin (**TPyP**) (400 MHz, $CDCl_3$)

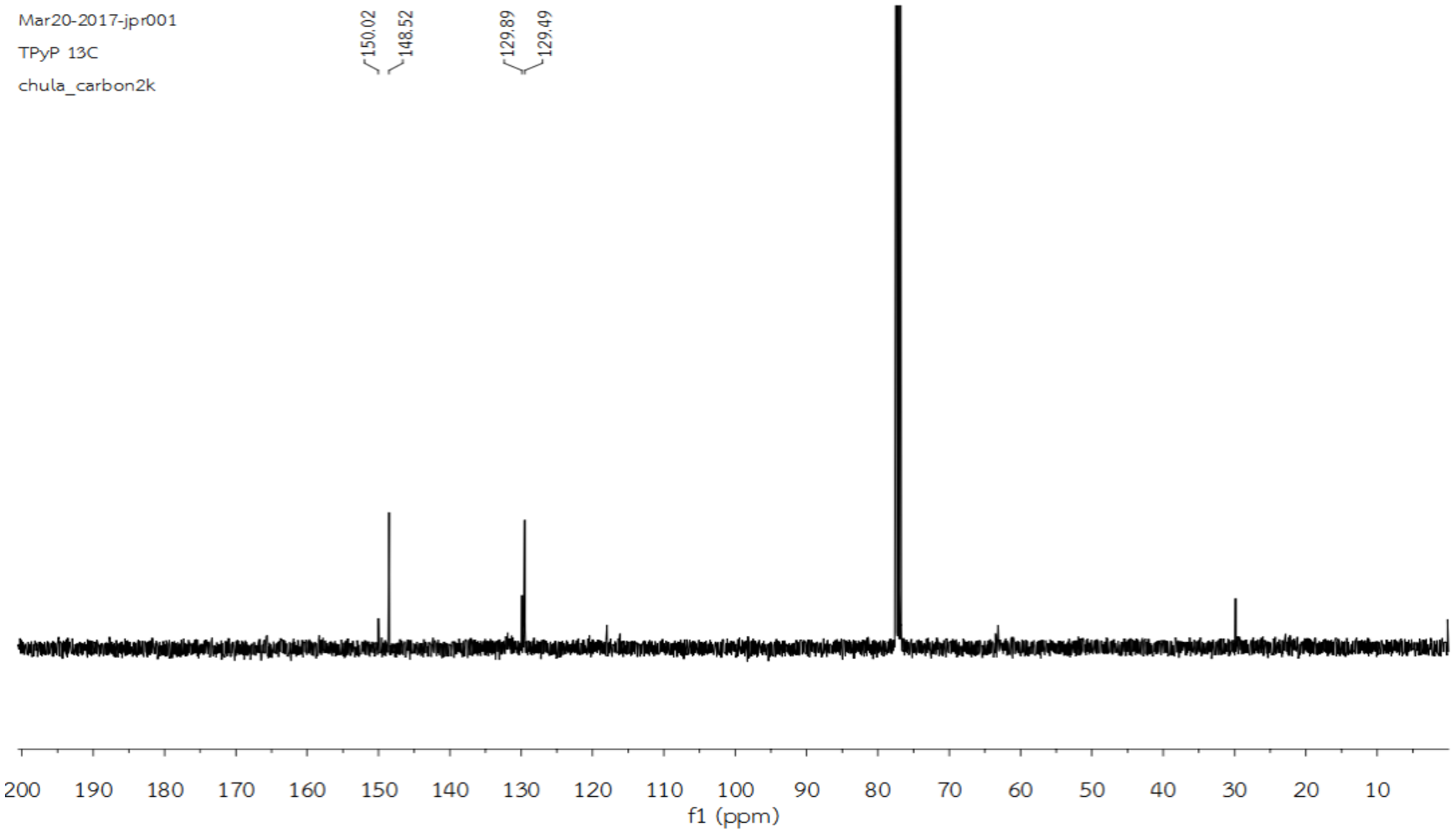

Figure 3.8 ^{13}C NMR of 5,10,15,20-tetrakis(4-pyridinyl)porphyrin (**TPyP**) (400 MHz, $CDCl_3$)

3.1.5 Synthesis and characterization of tetrakis(*N*-methyl-4-pyridinyl)porphine tetraiodide (TMPyP)

The synthesis of **TMPyP** was carried out *via* methylation reaction using **TPyP** react with methyl iodide in dimethylformamide (**Scheme 3.6**).[24] After precipitation process a dark brown solid of **TMPyP** iodonium salt was obtained in 93 %yield. The success was evidenced by the appearance of methyl protons at 4.73 ppm in its ^{1}H NMR spectrum (**Figure 3.9**). Moreover, ^{13}C NMR also showed the signal of methyl group at 47.94 ppm (**Figure 3.10)**. The mass spectrum showed fragment of $(\mathbf{M\text{-}CH_3})^{3+}$ at m/z = 221.312 suggested a loss of one methyl group from **TMPyP** (**Figure 3.11**).

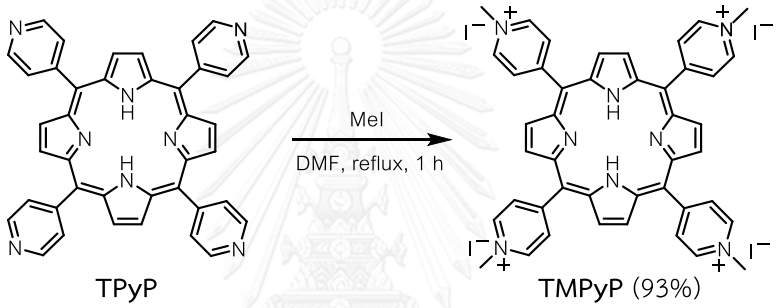

Scheme 3.6 Synthesis of tetrakis(*N*-methyl-4-pyridyl)porphine tetraiodide (**TMPyP**)

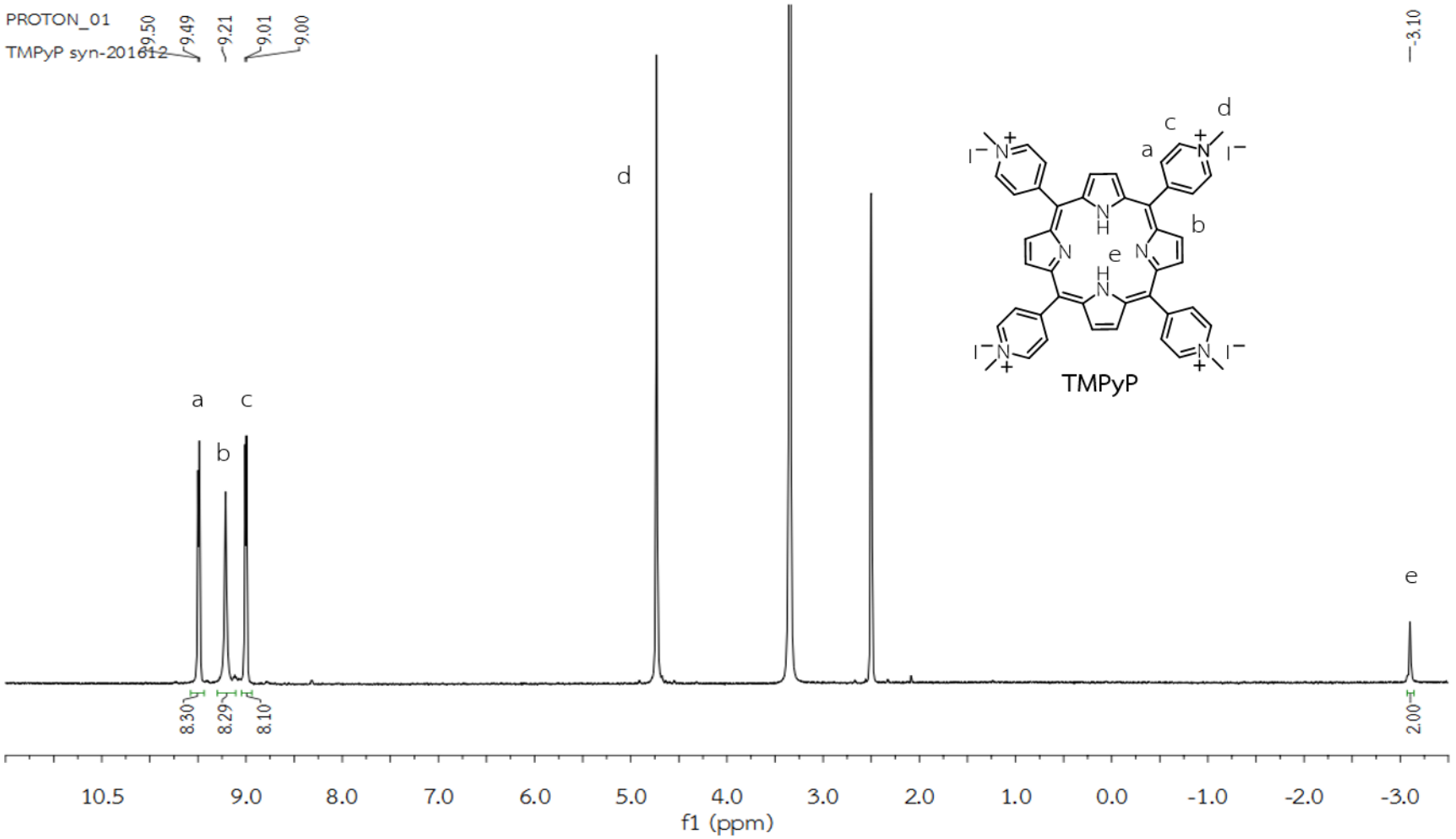

Figure 3.9 ^{1}H MNR of tetrakis(*N*-methyl-4-pyridyl)porphine tetraiodide (**TMPyP**) (400 MHz, DMSO-d_6)

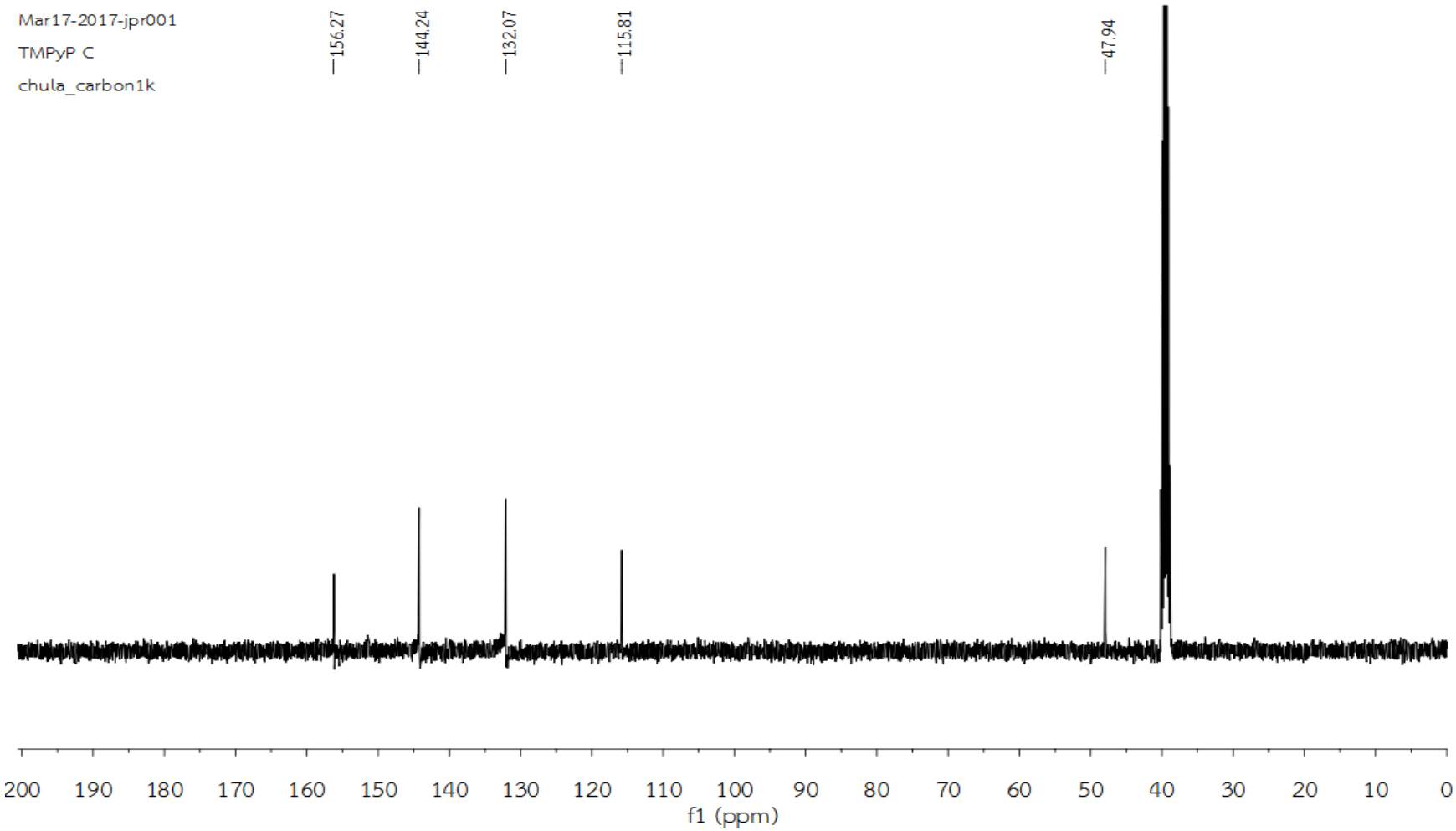

Figure 3.10 ^{13}C NMR of tetrakis(*N*-methyl-4-pyridyl)porphine tetraiodide (**TMPyP**) (400 MHz, DMSO-d_6)

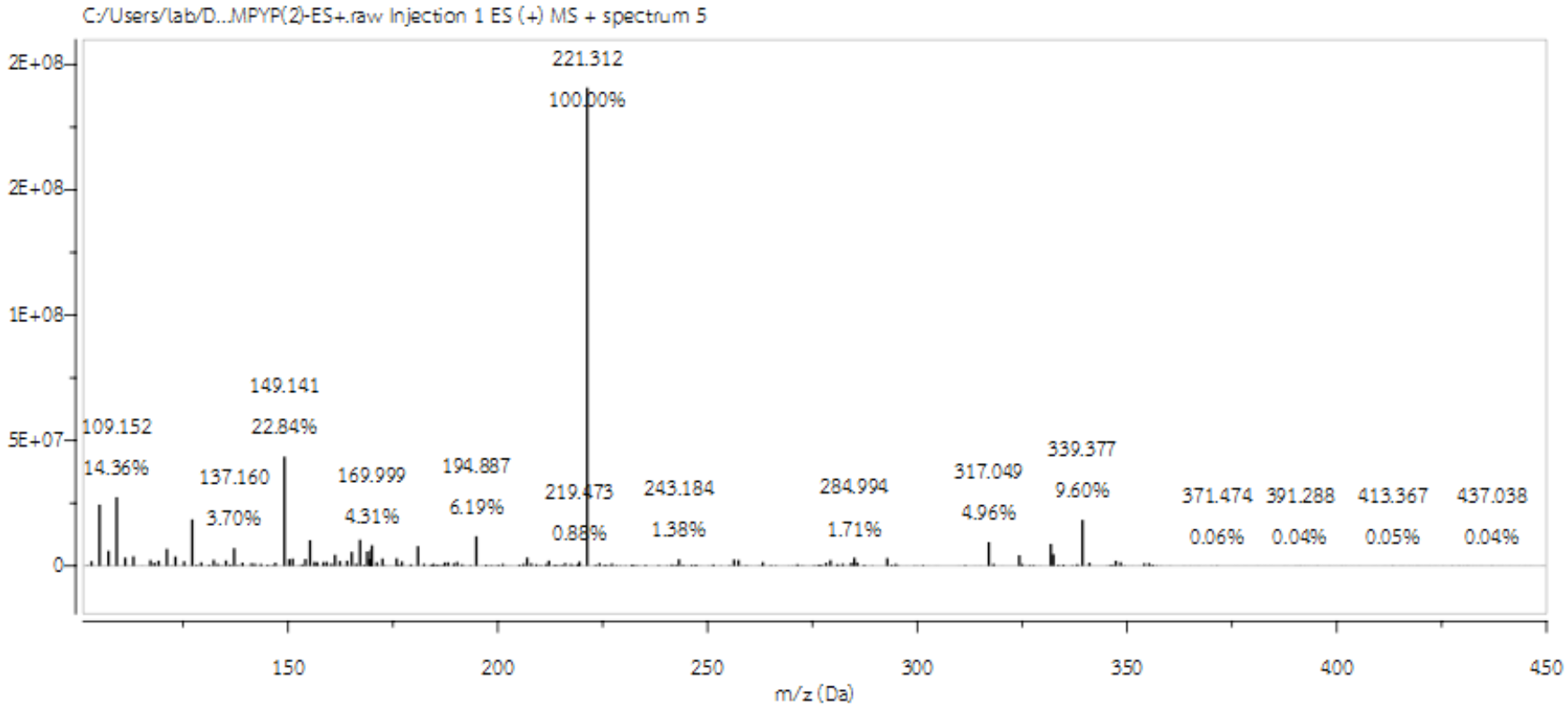

Figure 3.11 Mass spectrum of tetrakis(*N*-methyl-4-pyridyl)porphine tetraiodide (**TMPyP**)

3.2 Investigation of photophysical properties

3.2.1 UV-Vis absorption

The absorption spectra of **TPP**, **TSPP**, **TPyP** and **TMPyP** exbibited a characteristic absorption pattern of meso-substituted porphyrins, with absorption maxima at 411, 412, 412, and 421 nm, respectively (**Figure 3.12**). This absorption peak, which is also known as the Soret band or B-band, is caused by an electronic transition fron the zeroth singlet state to the second singlet excited state.[27] The red shift of soret band of **TMPyP** compared with **TPyP** was due to the positive charges of the pyridinium groups – this resulted in a delocalization of electrons in the **π-**conjugaed system of the porphyrin ring. There were also several absorption bands between 500-700 nm (Q band), which varied from one porphyrin to another.

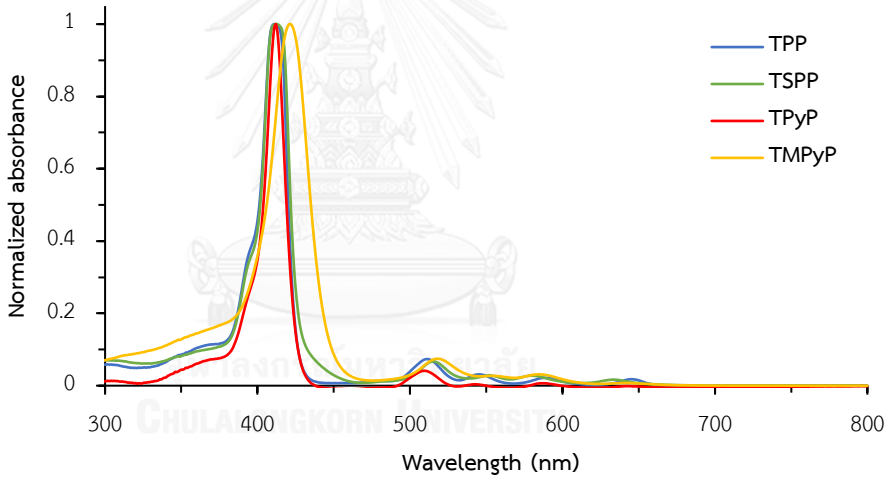

Figure 3.12 Absorption spectra of **TPP** (0.01 mM in 1% CH_2Cl_2-MeOH; λ_{max}= 411 nm), **TSPP** (0.01 mM in water; λ_{max}= 412 nm), **TPyP** (0.01 mM in 1% CH_2Cl_2-MeOH; λ_{max}= 412 nm) and **TMPyP** (0.01 mM in water; λ_{max}= 421 nm).

3.2.2 Fluorescence spectra

Fluorescence spectra of porphyrin derivertives are shown in **Figure 3.13.** Upon excitation at 411 nm, **TPP** exhibited two sharp emission peaks at 649 and 714 nm. With an excitation at 412 nm, **TSPP** exhibited emission peaks at 647 and 702 nm, while

TPyP exhibited emission peaks at 646 and 711 nm. **TMPyP** gave a broad emission peak at 710 nm upon the excitation at 421 nm.

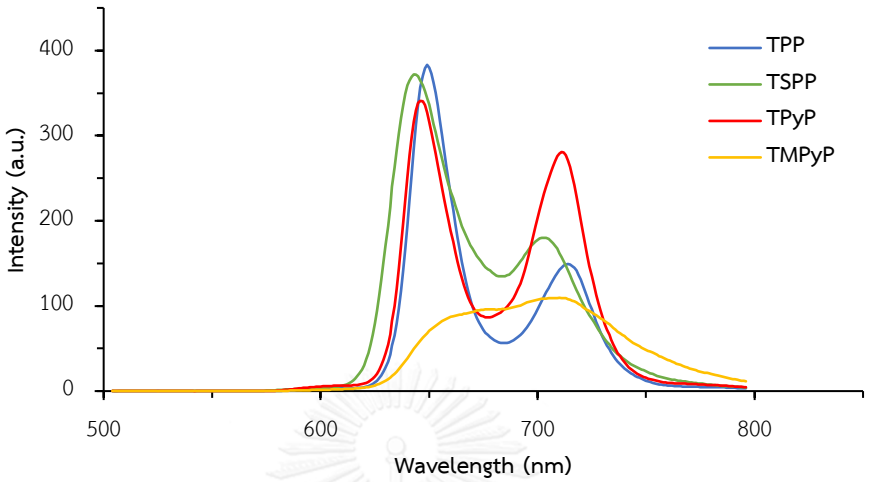

Figure 3.13 Emission spectra of **TPP** (0.01 mM in 1% CH_2Cl_2-MeOH; λ_{ex}= 411 nm), **TSPP** (0.01 mM in water; λ_{ex}= 412 nm), **TPyP** (0.01 mM in 1% CH_2Cl_2-MeOH; λ_{ex}= 412 nm) and **TMPyP** (0.01 mM in water; λ_{ex}= 421 nm).

3.3 Preliminary tests of charged porphyrin sensors

The selectivity of charged porphyrins for metal ions were investigated with a set of metal ions including K^+, Na^+, Ca^{2+}, Mg^{2+}, Cr^{3+}, Fe^{2+}, Cu^{2+}, Ni^{2+}, Zn^{2+}, Ag^+, Pb^{2+}, Hg^{2+} and Cd^{2+}.

There are many ways to create hydrophobic patterns on paper such as wax printing or permanent markers. Few reports demonstrated that permanent markers containing hydrophobic resin can be used to create hydrophobic patterns on paper.[14] In contrast, wax printing can be an efficient method to create complexed pattern on paper but the drawback is the requirement of a wax printer and computer software. For some experiments, such as undergraduate laboratory experiments, the use of permanent markers are more suitable. The hydrophobic wells acting as sensing zones were used for preliminary tests about the selectivity of charged porphyrins, where the mol ratio between porphyrin:metal ions was kept at 1:1 for simplicity. As expected

from previous reports, Hg^{2+} and Cd^{2+} gave distinguishable changes from the original pink color of **TSPP** to green, with Hg^{2+} being more obvious than Cd^{2+} (**Figure 3.14A**).

Focusing on **TMPyP**, this molecule gave a similar response with metal ions as did **TSPP**, but the original color was different. **TMPyP** gave discernible changes to Hg^{2+} and Cd^{2+} but with the color change from yellow to green (**Figure 3.14B**), while **TSPP** changed from pink to green. Pb^{2+} also showed slight change with both porphyrins.

Another important point worth mentioning is that pH has a profound effect on the complexation behavior of **TSPP**, which could be observed by naked eyes. For examples, several metal ions with the oxidation state of +3 are known to be prone to hydrolysis[28], resulting in higher concentrations of the hydronium ion and thus lower pH – this made **TSPP** turned green and confused the analysis. Therefore, a buffer solution was used in this study.

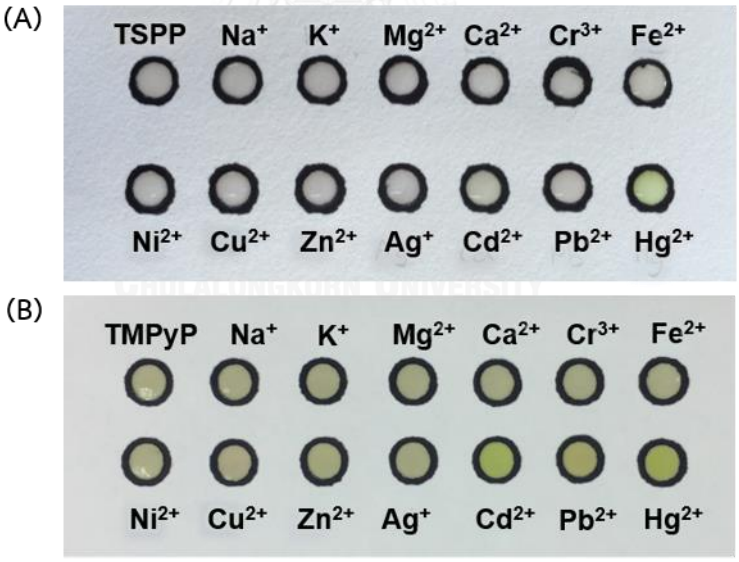

Figure 3.14 (A) Colorimetric changes of **TSPP** (0.10 mM in 2 mM HEPES buffer pH 7.5) and (B) **TMPyP** (0.10 mM in HEPES buffer pH 7.5) with a variety of metal ions (0.10 mM in 2 mM HEPES buffer pH 7.5).

Notably, the responses to metal ions in the fluorescence mode revealed that the fluorescence signals of both **TSPP** (0.1 mM) and **TMPyP** (0.1 mM) were completely quenched when Cu^{2+} (0.1 mM) was added. This phenomenon was found to be pretty selective as only Hg^{2+} and Cd^{2+} could also quench the fluorescence, albeit with a lesser degree. On the other hand, using higher concentration of certain metal ions such as Ag^{+} at 1 mM showed fluorescence decrease of the porphyrins. Therefore, the use of 0.1 mM for both of porphyrins and metal ions were justified.

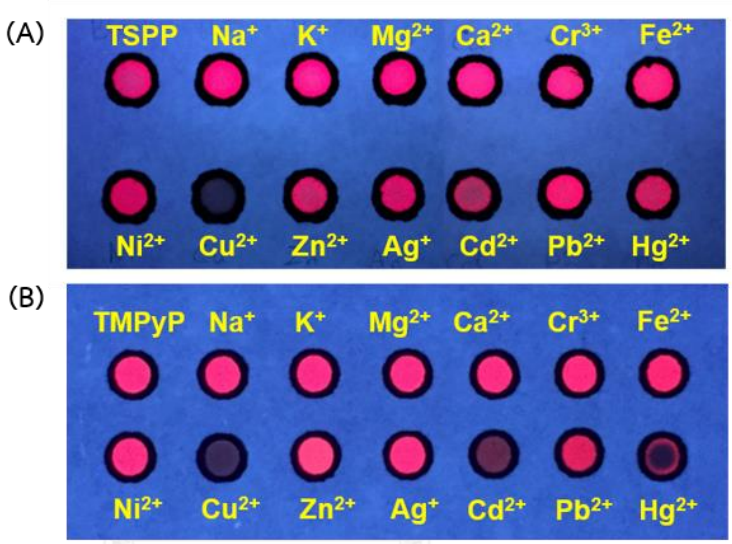

Figure 3.11 (A) Fluorometric changes of **TSPP** (0.10 mM in 2 mM HEPES buffer pH 7.5), (B) **TMPyP** (0.10 mM in 2 mM HEPES buffer pH 7.5) with variety of metal ions 0.10 mM in 2 mM HEPES buffer pH 7.5).

To evaluate qualitative ability of **TSPP** sensor, unknown samples consisting of more than one metal ion were tested with **TSPP** immobilized paper-based sensor. For example, unknown samples containing Hg^{2+} and Cu^{2+} revealed both colorimetric and fluorometric changes of **TSPP.** Moreover, unknown samples containing several ions without Hg^{2+} Cd^{2+} or Cu^{2+} could not change the color and fluorescence of **TSPP.**

As mentioned before, **TSPP** was selected to be used in practical organic chemistry course for a demonstration of the utilization of organic compounds in analytical chemistry. Undergraduate students in the practical organic course were required to synthesize their own batches of **TSPP.** This was followed by a simple

drawing of hydrophobic wells by permanent inks. **TSPP** and metal ions were then dropped in this confined region for testing. Moreover, students were asked to identify possible metal ions in unknown mixtures, it was found that all students could correctly identify the mixtures that contain Hg^{2+} and Cu^{2+} (**Figure 3.12**).

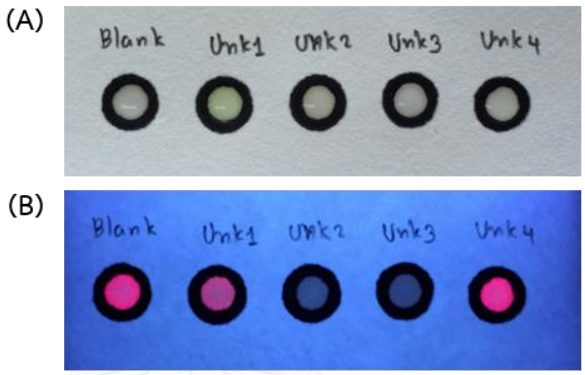

Figure 3.12 (A) Colorimetric changes and (B) Fluorometric change of **TSPP** with unknown samples including unk 1: Hg^{2+}, Ca^{2+}, Pb^{2+}; Unk 2: Hg^{2+}, Cu^{2+}; Unk 3: Cu^{2+}, Zn^{2+}; Unk 4: Pb^{2+}, Ca^{2+}, Zn^{2+} (concentration of each metal in all samples were 0.1 mM). Images were from student's results.

On the other hand, due to the fact that **TMPyP** tended to retain well on paper even after aqueous washing, it was selected to study the sensitivity of **TMPyP** for Cu^{2+} sensing and to create a prototype of a portable microfluidic distance-based paper device.

3.4 Sensitivity of TMPyP for Cu^{2+} sensor

To evaluate the sensitivity of **TMPyP** for Cu^{2+} sensing, a calibration curve was created using a Cu^{2+} concentration series from 1 to 100 μM. Fluorescence images of **TMPyP** immobilized paper with various concentrations of Cu^{2+} ion were shown in **Figure 3.13A**. A calibration curve was obtained by plotting normalized mean intensity of gray values (converted by the ImageJ software) versus the standard concentrations of Cu^{2+} ion. The calibration curve showed a linear range of Cu^{2+} concentration from 1 to 20 μM. The quenching appeared to be virtually complete at 20 μM and beyond, matching well with the fact that the concentration of **TMPyP** was also 20 μM (assuming

1:1 binding ratio). Moreover, the limit of detection was determined and calculated using 3 times of signal to noise ratio. From the calibration curve in **Figure 3.13B**, the limit of detection was calculated to be 0.15 μM. Since the Environment Protection Agency (EPA) imposed an upper limit of copper in drinking water to be 1.3 ppm (20.5 μM),[29] our paper device was clearly able to measure Cu^{2+} in drinking water.

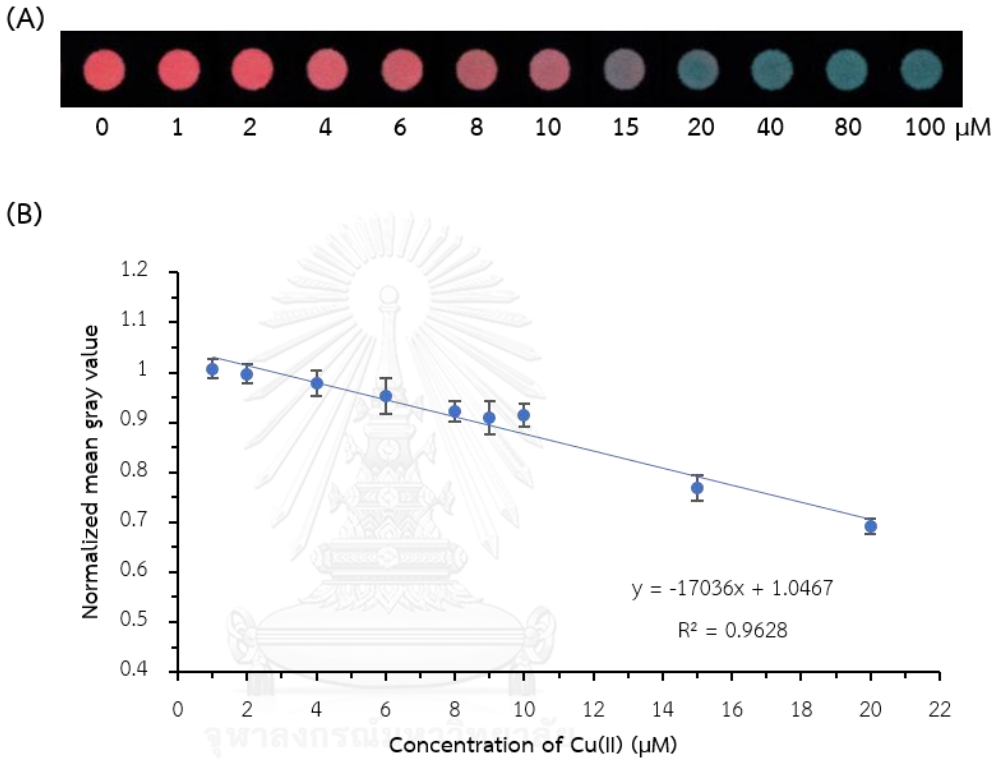

Figure 3.13 (A) Fluorescence images of the **TMPyP** (20 μM in 0.2 M acetate buffer pH 5.0) with different concentrations of Cu^{2+} (0-100 μM). (B) Plot of normalized mean gray intensity versus Cu^{2+} concentrations from 0 to 20 μM.

3.5 Interference tolerance tests

For interference tolerance studies, a set of metal ions including K^{+}, Na^{+}, Ca^{2+}, Mg^{2+}, Cr^{3+}, Fe^{2+}, Ni^{2+}, Zn^{2+}, Ag^{+}, Pb^{2+}, Hg^{2+} and Cd^{2+} were used in this study. Each metal ions was mixed with 10 μM of Cu^{2+} solution with the molar ratio between copper:other ions at 1:1 and 1:10. Then, the mixture was separately dropped onto **TMPyP** (20 μM

in 0.2 M acetate buffer pH 5.0) wells. The data were shown in **Figure 3.14** as normalized mean gray values.

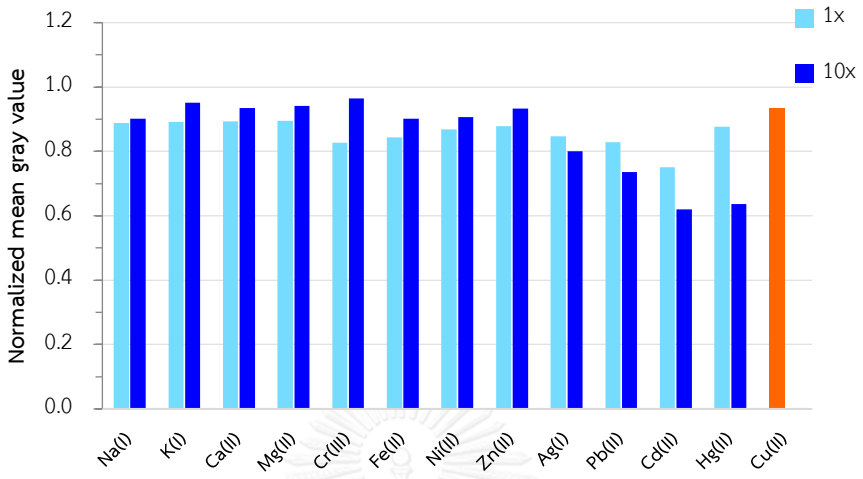

Figure 3.14 Interference tolerant studies of the mixture of various metals ion with 10 μM of Cu^{2+} at 1:1 and 1:10 molar ratio of copper:other ions. The data was collected converted to numerical values from fluorescence images *via* the ImageJ software.

The results found that fluorescence signals from 1:1 and 1:10 ratio of K^{+}, Na^{+}, Ca^{2+}, Mg^{2+}, Cr^{3+}, Fe^{2+}, Ni^{2+} and Zn^{2+} could not interfere the binding between Cu^{2+} and **TMPyP** with the percent differences of less than 10% compared with the control solution. On the other hand, Ag^{+} and Hg^{2+} significantly interfered the TMPyP-Cu^{2+} interaction at the ratio of 1:10 (**Figure 3.14**). In addition, Cd^{2+} and Pb^{2+} significantly interfered the device **TMPyP**-Cu^{2+} interaction at the ratio of 1:1.

3.6 Evaluation of Cu^{2+} levels in real water sample

To evaluate the ability of the device in the real world, two commercial mineral water samples and tap water were spiked with Cu^{2+} to two concentrations (5 μM and 20 μM). Then, the water samples were dropped onto porphyrin-immobilized wells containing 20 μM of **TMPyP** in acetate buffer pH 5.0. The data was collected with the ImageJ software and used to calculate the recovery concentration using the calibration curve in **Figure 3.13**.

Table 3.1 Measurements of Cu^{2+} in spiked water samples

sample	Cu^{2+} (μM)		% recovery
	added	found	
Drinking water A	0	not detected	-
	5	4.8±1.3	96 ±28
	20	20.2±1.4	100 ±7
Drinking water B	0	not detected	-
	5	4.9 ± 0.8	98 ± 15
	20	18.9 ± 1.2	94 ± 7
Tap water	0	not detected	-
	5	4.9 ± 0.9	98 ± 17
	20	19.7 ± 0.9	99 ± 5

The amounts of Cu^{2+} in spiked samples determined using **TMPyP**-immobilized were shown in **Table 3.1**. All water samples without further spiking was also determined by ICP-OES and found no Cu^{2+}. Moreover, the spiking results revealed that the percentage of recoveries were in the range of 94-100%, which was an acceptable recovery according to the AOAC guideline[30] - the recovery would be in the range of 80-110% for an analyte concentration 0.0001% (w/w). The amounts of Cu^{2+} in spiked samples will be determined by the ICP-OES method as a means to benchmark the sensor fabricated in this study.

3.7 Application of TMPyP sensor as a distance-based paper device

With a relatively good retention on paper, **TMPyP** was used to test whether a **TMPyP** immobilized microfluidic distance-based paper device could be developed. The hydrophobic pattern and the ruler scale were absorbed on chromatography paper with molten wax. Thereafter, 0.5 mM of **TMPyP** in 0.2 M acetate buffer pH 5 was deposited along the detection channel by inkjet printer. In this work, the detection channel width was varied to optimize the quenching range of porphyrin. The results in **Figure 3.16** indicated that increasing the channel width led to a shorter length of quenching, due to the increasing porphyrin molecules to be quenched per length unit.

Thus, the differentiation power of lower concentrations of Cu^{2+} was greater in the narrow channel (0.5 mm). Nevertheless, the wider channel (2 mm) required a shorter time for wicking liquid to the end of the channel resulting in a reduction of the analysis time. To balance between the differentiation power and the analysis time, the width of 1 mm was deemed suitable for determining the amount of Cu^{2+} in this work.

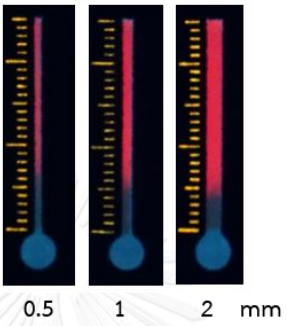

Figure 3.16 Effect of the channel dimensions to the wicking behavior of the sensor.

To demonstrate the use of the distance-based device in the real situation, the dynamic range for Cu^{2+} sensing was studied. 20 µL of various concentrations of Cu^{2+} in the range of 8 to 36 ppm was dropped on the detection reservoir. After the solution traveled along the detection channel and then dried, the quenching range of porphyrin was measured. The preliminary results in **Figure 3.17** revealed that the distance-based device able to differentiate the quenching range of each concentration of Cu^{2+}. For further modification in the future, the ruler mark would be replaced by a concentration mark for simple read-out by unskilled users.

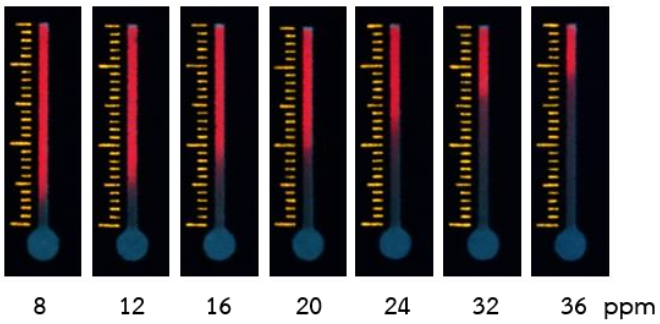

Figure 3.17 Fluorescence images of **TMPyP** immobilized microfluidic distance-based paper device with different concentrations of Cu^{2+} (8-36 ppm)

CHAPTER IV
CONCLUSION

Herein, charged porphyrins including tetrakis(4-sulfonatophenyl)porphyrin (**TSPP**) and tetrakis(*N*-methyl-4-pyridyl)porphine tetraiodide (**TMPyP**) were synthesized and studied for its ability for heavy metal sensing. Focusing on **TSPP**, the molecule revealed clear colorimetric changes after adding Hg^{2+} and Cd^{2+}, by both giving with the change from pink to green color. Moreover, the fluorescence of **TSPP** was completely quenched by Cu^{2+}. **TSPP** was successfully applied as a learning topic in practical organic chemistry course as an example for the integration between organic synthesis and analytical chemistry. On the other hand, the color changes of **TMPyP** was roughly similar to **TSPP**, with the color change from yellow to green in Hg^{2+} and Cd^{2+} sensings. Fluorescence of **TMPyP** was quenched by Cu^{2+}. With its strong retention on paper, **TMPyP** was used for the fabrication of fluorescence microfluidic distance-based paper device for Cu^{2+} detection. The quantitative study showed that the **TMPyP**-immobilized paper device could detect Cu^{2+} with the limit of detection of 0.15 μM. In addition, the device was successfully used to determine amounts of Cu^{2+} in spiked water sample with the percent recovery in the range of 94-100%. Moreover, distance-based microfluidic paper devices based on fluorescence quenching were developed and could detect Cu^{2+} in the range of 13 to 57 μM (8 to 36 ppm of Cu^{2+})

REFERENCES

References:

1. Järup, L., Hazards of Heavy Metal Contamination. *Br. Med. Bull.* **2003,** *68* (1), 167-182.

2. Lemos, V. A.; Carvalho, A. L., Determination of Cadmium and Lead in Human Biological Samples by Spectrometric Hechniques: a Review. *Environ. Monit. Assess.* **2009,** *171* (1), 255-265.

3. Brewer, G. J., Risks of Copper and Iron Toxicity during Aging in Humans. *Chem. Res. Toxicol.* **2010,** *23* (2), 319-326.

4. Aragay, G.; Pons, J.; Merkoçi, A., Recent Trends in Macro-, Micro-, and Nanomaterial-Based Tools and Strategies for Heavy-Metal Detection. *Chem. Rev.* **2011,** *111* (5), 3433-3458.

5. Jiang, X.; Fan, Z. H., Fabrication and Operation of Paper-Based Analytical Devices. *Annu. Rev. Anal. Chem* **2016,** *9* (1), 203-222.

6. Mentele, M. M.; Cunningham, J.; Koehler, K.; Volckens, J.; Henry, C. S., Microfluidic Paper-Based Analytical Device for Particulate Metals. *Anal. Chem.* **2012,** *84* (10), 4474-4480.

7. Han, W. S.; Lee, H. Y.; Jung, S. H.; Lee, S. J.; Jung, J. H., Silica-Based Chromogenic and Fluorogenic Hybrid Chemosensor Materials. *Chem. Soc. Rev.* **2009,** *38* (7), 1904-1915.

8. Kim, H. N.; Ren, W. X.; Kim, J. S.; Yoon, J., Fluorescent and Colorimetric Sensors for Detection of Lead, Cadmium, and Mercury Ions. *Chem. Soc. Rev.* **2012,** *41* (8), 3210-3244.

9. Li, M.; Cao, R.; Nilghaz, A.; Guan, L.; Zhang, X.; Shen, W., "Periodic-Table-Style" Paper Device for Monitoring Heavy Metals in Water. *Anal. Chem.* **2015,** *87* (5), 2555-2559.

10. Balaji, T.; Sasidharan, M.; Matsunaga, H., Optical Sensor for The Visual Detection of Mercury Using Mesoporous Silica Anchoring Porphyrin Moiety. *Analyst* **2005,** *130* (8), 1162-1167.

11. Srivastava, P.; Razi, S. S.; Ali, R.; Gupta, R. C.; Yadav, S. S.; Narayan, G.; Misra, A., Selective Naked-Eye Detection of Hg^{2+} through an Efficient Turn-On Photoinduced Electron Transfer Fluorescent Probe and Its Real Applications. *Anal. Chem.* **2014,** *86* (17), 8693-8699.

12. Takahashi, Y.; Kasai, H.; Nakanishi, H.; Suzuki, T. M., Test Strips for Heavy-Metal Ions Fabricated from Nanosized Dye Compounds. *Angew. Chem. Int. Ed.* **2006,** *45* (6), 913-916.

13. Lee, S. J.; Lee, J. E.; Seo, J.; Jeong, I. Y.; Lee, S. S.; Jung, J. H., Optical Sensor Based on Nanomaterial for the Selective Detection of Toxic Metal Ions. *Adv. Funct. Mater.* **2007,** *17* (17), 3441-3446.

14. Xu, C.; Cai, L.; Zhong, M.; Zheng, S., Low-cost and rapid prototyping of microfluidic paper-based analytical devices by inkjet printing of permanent marker ink. *RSC Adv* **2015,** *5* (7), 4770-4773.

15. Meredith, N. A.; Quinn, C.; Cate, D. M.; Reilly, T. H.; Volckens, J.; Henry, C. S., Paper-based analytical devices for environmental analysis. *Analyst* **2016**.

16. Cate, D. M.; Dungchai, W.; Cunningham, J. C.; Volckens, J.; Henry, C. S., Simple, distance-based measurement for paper analytical devices. *Lab Chip* **2013,** *13* (12), 2397-2404.

17. Yamada, K.; Henares, T. G.; Suzuki, K.; Citterio, D., Distance-Based Tear Lactoferrin Assay on Microfluidic Paper Device Using Interfacial Interactions on Surface-Modified Cellulose. *ACS Appl. Mater. Interfaces* **2015,** *7* (44), 24864-24875.

18. Cate, D. M.; Noblitt, S. D.; Volckens, J.; Henry, C. S., Multiplexed paper analytical device for quantification of metals using distance-based detection. *Lab Chip* **2015,** *15* (13), 2808-2818.

19. Tian, T.; Li, J.; Song, Y.; Zhou, L.; Zhu, Z.; Yang, C. J., Distance-based microfluidic quantitative detection methods for point-of-care testing. *Lab Chip* **2016,** *16* (7), 1139-1151.

20. Biesaga, M.; Pyrzyńska, K.; Trojanowicz, M., Porphyrins in Analytical Chemistry. A Review. *Talanta* **2000,** *51* (2), 209-224.

21. El-Safty, S. A.; Prabhakaran, D.; Ismail, A. A.; Matsunaga, H.; Mizukami, F., Nanosensor Design Packages: A Smart and Compact Development for Metal Ions Sensing Responses. *Adv. Funct. Mater.* **2007,** *17* (18), 3731-3745.

22. Adler, A. D.; Longo, F. R.; Finarelli, J. D.; Goldmacher, J.; Assour, J.; Korsakoff, L., A simplified synthesis for meso-tetraphenylporphine. *J. Org. Chem.* **1967,** *32* (2), 476-476.

23. Dong, Z.; Scammells, P. J., New Methodology for the N-Demethylation of Opiate Alkaloids. *J. Org. Chem.* **2007,** *72* (26), 9881-9885.

24. Berezin, M. B.; Berezina, N. M.; Semeikin, A. S.; V'yugin, A. I., Thermochemistry of solution of some quaternized derivatives of tetra(4-pyridyl)porphine in water. *Russ. J. Gen. Chem.* **2006,** *77* (11), 1955-1958.

25. Rothemund, P., FORMATION OF PORPHYRINS FROM PYRROLE AND ALDEHYDES. *J. Am. Chem. Soc.* **1935,** *57* (10), 2010-2011.

26. Lindsey, J. S.; Schreiman, I. C.; Hsu, H. C.; Kearney, P. C.; Marguerettaz, A. M., Rothemund and Adler-Longo reactions revisited: synthesis of tetraphenylporphyrins under equilibrium conditions. *J. Org. Chem.* **1987,** *52* (5), 827-836.

27. L. Anderson, H., Building molecular wires from the colours of life: conjugated porphyrin oligomers. *Chem. Commun.* **1999,** (23), 2323-2330.

28. Devis, K. W.; Peck, R. E.; Stanley, G. G., *Chemistry*. Brooks Cole: 2010; Vol. 9.

29. Environmental; Protection; Agency Lead and Copper Rule. https://www.epa.gov/dwreginfo/lead-and-copper-rule (accessed 1 May 2017).

30. AOAC; International appendix f: guidelines for standard method performance requirements. http://www.eoma.aoac.org/app_f.pdf.

APPENDIX

VITA

Miss Jutamat Prabphal was born on 12th of May, 1992 in Nakorn Nayok, Thailand. She graduated Bachelor's Degree in chemistry with first class honors from faculty of science at Chulalongkorn University, Bangkok in 2014. Then, she was admitted into a Master Degree in the major of Chemistry, Faculty of Science, chulalongkorn University, Bangkok in 2014 and completed the program in 2017.